Published for SISSA by Springer

Received: October 7, 2025
Accepted: November 1, 2025
Published: January 26, 2026

Measurement of the branching fraction of the $\Lambda_b^0 \to J/\psi \Lambda$ decay and isospin asymmetry of $B \to J/\psi K$ decays

The LHCb collaboration

R. Aaij et al.

Full author list at the end of the paper

E-mail: lgarciam@cern.ch

Abstract: This paper describes a measurement of the $\Lambda_b^0 \to J/\psi \Lambda$ branching fraction using data collected with the LHCb experiment in proton-proton collisions from 2016 to 2018. The dataset corresponds to an integrated luminosity of 5.4 fb^{-1}. The branching fraction is determined relative to that of $B^0 \to J/\psi K_S^0$ decays,

$$\frac{\mathcal{B}(\Lambda_b^0 \to J/\psi \Lambda)}{\mathcal{B}(B^0 \to J/\psi K_S^0)} = 0.750 \pm 0.005 \pm 0.022 \pm 0.005 \pm 0.062\,,$$

yielding $\mathcal{B}(\Lambda_b^0 \to J/\psi \Lambda) = (3.34 \pm 0.02 \pm 0.10 \pm 0.08 \pm 0.28) \times 10^{-4}$, where the first uncertainty is statistical, the second systematic, the third due to external inputs on branching fractions and the fourth due to the ratio of Λ_b^0 baryon and B^0 meson hadronisation fractions. In addition, the isospin asymmetry between the rates of $B^0 \to J/\psi K_S^0$ and $B^+ \to J/\psi K^+$ decays is measured to be

$$A_{\rm I} = -0.0135 \pm 0.0004 \pm 0.0133\,,$$

where the first uncertainty is statistical and the second systematic.

Keywords: B Physics, Branching fraction, Flavour Physics, Hadron-Hadron Scattering

ArXiv ePrint: 2509.12805

https://doi.org/10.1007/JHEP01(2026)159

JHEP01(2026)159

Contents

JHEP01(2026)159

1 Introduction

Decays of b hadrons to final states with J/ψ mesons provide clean experimental signatures that have been used extensively to calibrate measurements at the B-factory experiments, the LHC and the Tevatron. At the Tevatron and the LHC, these decays have also played an important role in normalising event yields in analyses of rare or forbidden processes, such as the $B_s^0 \to \mu^+\mu^-$ decay [1–4]. The branching fractions of the $B^0 \to J/\psi K_S^0$ and $B^+ \to J/\psi K^+$ decays are known precisely from measurements by the BaBar, Belle and CLEO experiments [5–10].[1] The branching fractions of b-baryon decays to final states with J/ψ mesons are known much less precisely as b baryons are not producible in the B-factory experiments. At the Tevatron, the D0 [11] and CDF [12] experiments have measured the product of the fraction of b quarks that hadronise to form a Λ_b^0 baryon and the branching fraction of the $\Lambda_b^0 \to J/\psi \Lambda$ decay, $f(b \to \Lambda_b^0) \times \mathcal{B}(\Lambda_b^0 \to J/\psi \Lambda)$. The Λ_b^0 production fraction is known to be strongly p_{T}-dependent and different assumptions on $f(b \to \Lambda_b^0)$ have a significant impact on the determination of $\mathcal{B}(\Lambda_b^0 \to J/\psi \Lambda)$ [13]. The p_{T} dependence of $f(b \to \Lambda_b^0)$ has been studied by the LHCb collaboration in pp collisions at the LHC [14, 15], allowing for a more precise determination of $\mathcal{B}(\Lambda_b^0 \to J/\psi \Lambda)$.

This paper describes a measurement of the $\Lambda_b^0 \to J/\psi \Lambda$ branching fraction using a dataset collected by the LHCb experiment from 2016 to 2018 in proton-proton collisions at a centre-of-mass energy of $\sqrt{s} = 13\,\mathrm{TeV}$. The dataset corresponds to an integrated luminosity of $5.4\,\mathrm{fb}^{-1}$. To account for the p_{T} dependence of the b-hadron production, and to validate the

[1] The inclusion of charge-conjugate processes is implied throughout.

analysis procedure, the data are analysed in bins of p_{T} using intervals of $1\,\mathrm{GeV}/c$ in the range $[4, 14]\,\mathrm{GeV}/c$ and $2\,\mathrm{GeV}/c$ in the range $[14, 20]\,\mathrm{GeV}/c$. The observed yields of $\Lambda_b^0 \to J/\psi\Lambda$ decays are normalised with respect to those of $B^0 \to J/\psi K^0_{\mathrm{S}}$ decays, exploiting the similar topology of the two decays in the detector when the K^0_{S} meson and Λ baryon are reconstructed through the decays $K^0_{\mathrm{S}} \to \pi^+\pi^-$ and $\Lambda \to p\pi^-$.

A comparison of the rates of $B^+ \to J/\psi K^+$ and $B^0 \to J/\psi K^0_{\mathrm{S}}$ decays as a function of the B-meson p_{T} is used to validate the reconstruction and selection of the long-lived hadrons in the LHCb detector. In the Standard Model, it is expected that the partial widths of the $B^+ \to J/\psi K^+$ and $B^0 \to J/\psi K^0$ decays are almost identical, as the only difference between the decays is the flavour of the light spectator quark (see e.g. ref. [16]). The resulting isospin asymmetry,

$$A_{\mathrm{I}}[B \to J/\psi K] = \frac{\frac{\tau_{B^+}}{\tau_{B^0}}\mathcal{B}(B^0 \to J/\psi K^0) - \mathcal{B}(B^+ \to J/\psi K^+)}{\frac{\tau_{B^+}}{\tau_{B^0}}\mathcal{B}(B^0 \to J/\psi K^0) + \mathcal{B}(B^+ \to J/\psi K^+)}\,, \tag{1.1}$$

where $\tau_{B^+}/\tau_{B^0} = 1.076 \pm 0.004$ [17] is the ratio between the B^+ and B^0 meson lifetimes, is expected to be zero. Previous measurements of A_{I} by the Belle [5] and Belle II [18] collaborations and the reinterpretation of BaBar and Belle data in ref. [19] are consistent with this expectation. In this analysis, A_{I} is determined from the $B^+ \to J/\psi K^+$ and $B^0 \to J/\psi K^0_{\mathrm{S}}$ samples assuming $\mathcal{B}(B^0 \to J/\psi K^0_{\mathrm{S}}) = \frac{1}{2}\mathcal{B}(B^0 \to J/\psi K^0)$. Kaon regeneration in detector material, and neutral-kaon mixing modify this assumption at the per-mille level [20]. It is assumed that $f(b \to B^0)$ and $f(b \to B^+)$ are equal for pp collisions at $\sqrt{s} = 13\,\mathrm{TeV}$.

2 Detector and simulation

The LHCb detector [21, 22] is a single-arm forward spectrometer covering the pseudorapidity range $2 < \eta < 5$, designed for the study of particles containing b or c quarks. The detector elements that are particularly relevant to this analysis are: a silicon-strip vertex detector surrounding the proton-proton interaction region that allows c and b hadrons to be identified from their characteristically long flight distance; a tracking system that provides a measurement of the momentum, p, of charged particles; two ring-imaging Cherenkov detectors (referred to as RICH 1 and RICH 2) that are able to discriminate between different species of charged hadrons; an electromagnetic calorimeter to reconstruct electron and photon energy deposits; a muon system to identify muons. Events are selected online using a trigger [23, 24] that comprises a hardware and a software stage. In preparation for analysis, they undergo a centralised, offline processing step to deliver physics-analysis-ready data across the entire LHCb physics programme [25].

Simulated samples are used to determine the efficiency of the candidate selection as well as the distributions of specific sources of background. In the simulation, pp collisions are generated using Pythia [26] with a specific LHCb configuration [28]. Decays of unstable particles are described by EvtGen [29], using Photos [30] to generate final-state radiation. The interactions of the generated particles with the detector, and its response, are simulated using the Geant4 toolkit [31] as described in ref. [33]. The simulated samples are corrected to account for known differences between simulation and data. Corrections are applied to the

JHEP01(2026)159

simulated tracking and particle-identification performance, and to the production kinematics of the b hadrons. The kinematic corrections are derived from $B^+ \to J/\psi K^+$ decays that satisfy the candidate selection procedure described below. It is assumed that B^0 and B^+ mesons are produced with the same kinematic distributions. The measured hadronisation fractions from refs. [14, 15] are used to derive kinematic corrections for Λ_b^0 baryons from those of B^+ mesons. The angular distributions of simulated $\Lambda_b^0 \to J/\psi \Lambda$ decays are weighted to reproduce those in ref. [34].

3 Candidate selection

At the hardware trigger level, events are selected if they contain at least one high-p_{T} muon. In the software trigger, at least one muon is required to have a large p_{T} and a large impact parameter (IP) with respect to every pp interaction point (PV). Further, events are required to contain a pair of opposite-charge muons that are displaced from every PV.

In the offline selection, B^+, B^0 and Λ_b^0 candidates are formed by combining a muon pair consistent with originating from the decay of a J/ψ meson with a K^+ meson, K_S^0 meson, or Λ baryon candidate, respectively. The J/ψ, K_S^0 and Λ candidates are required to have masses in the ranges $[3030, 3150]\,\mathrm{MeV}/c^2$, $[468, 528]\,\mathrm{MeV}/c^2$ and $[1105, 1125]\,\mathrm{MeV}/c^2$, respectively. The K_S^0 and Λ candidates are formed from two opposite-charge tracks and are split into two categories depending on whether or not the tracks are reconstructed in the vertex detector: tracks reconstructed with (without) segments in the vertex detector are categorised as *long* (*downstream*). Candidates in the long (downstream) category are required to have a decay vertex displaced along the beam axis from the origin of the experiment's coordinate system by less than 400 mm (2250 mm), to ensure they are well reconstructed. The motivation for these requirements is twofold: long-category candidates with displacements larger than 400 mm leave only a small number of hits in the vertex detector, making their reconstruction efficiency highly sensitive to detector inefficiencies, while downstream-category candidates with displacements beyond 2250 mm are affected by material interactions at the interface between RICH 1 and the tracking system. The K^+ candidate is required to be positively identified as a kaon by the detector's particle-identification systems. No particle-identification requirements are applied to the tracks used to form the K_S^0 and Λ candidates, as the narrow mass window requirements around the known K_S^0 and Λ masses [35] reduce the level of cross-feed background from K_S^0 mesons identified as Λ baryons, and vice versa, to a manageable level. All reconstructed tracks are required to have a significant IP with respect to every PV in the event. The $\pi^+\pi^-$, $p\pi^-$ and $\mu^+\mu^-$ candidates are required to be consistent with originating from vertices corresponding to the decays of the K_S^0 meson, Λ baryon or J/ψ meson, respectively. The decay products of the b hadron are also required to be consistent with originating from a single point. The b-hadron candidate is required to be displaced from every PV in the event and be consistent with originating from a PV. To improve the resolution on the reconstructed b-hadron mass, a kinematic fit is performed [36] that constrains the J/ψ mass and K_S^0 or Λ mass to their known values [35], and constrains the b hadron to originate from its associated PV, defined as the PV with the smallest IP with respect to the b-hadron candidate.

JHEP01(2026)159

Gradient-boosted decision-tree classifiers [37] are used to further suppress combinatorial background, where tracks from multiple different sources are combined, in the B^0 and Λ_b^0 long-category datasets. This is not necessary for the downstream-category datasets, which already have good signal purity. A separate classifier is trained for each dataset, using B^0 and Λ_b^0 candidates from simulation as a signal proxy and data candidates with a b-hadron mass in the high-mass range $[5900, 7000]\,\text{MeV}/c^2$ as a background proxy. The classifier uses information on the displacement of the K^0_S/Λ and the b-hadron candidates from their associated PVs, the K^0_S/Λ p_T, the vertex-fit quality of the b-hadron candidate and the angle between its momentum vector and the vector connecting its production and decay vertices. The working points of the classifiers are chosen to maximise the expected statistical significances of the B^0 and Λ_b^0 signals in the data. The expected signal yield at each working point is obtained by scaling the yield without any classifier requirement by the relative efficiency of the working point in simulation. The expected background yield is determined from a fit to the upper-mass sideband region of the data. After applying the full selection procedure, 99% of the selected events contain only a single b-hadron candidate. If more than one candidate is reconstructed in an event, a single candidate is selected arbitrarily.

In addition to combinatorial background, the other sources of background in the selected samples are: $\Lambda_b^0 \to J/\psi\Lambda$ ($B^0 \to J/\psi K^0_\text{S}$) decays that are reconstructed as $B^0 \to J/\psi K^0_\text{S}$ ($\Lambda_b^0 \to J/\psi\Lambda$) decays in the B^0 (Λ_b^0) sample; $B^+ \to J/\psi\pi^+$ decays where the pion is misidentified as a kaon in the B^+ sample; $B^0_s \to J/\psi K^0_\text{S}$ decays in the B^0 sample; and $\Xi_b{}^{+,0} \to J/\psi\Xi^{+,0}$ decays, where the $\Xi^{+,0}$ baryon decays to $\Lambda\pi^{+,0}$ and the pion is not reconstructed, in the Λ_b^0 sample. It is also possible for Ξ_b^0 baryons to decay directly to $J/\psi\Lambda$, but the branching fraction of this process is sufficiently small, $\mathcal{B}(\Xi_b^0 \to J/\psi\Lambda)/\mathcal{B}(\Xi_b^0 \to J/\psi\Xi^0) = (8.2 \pm 2.1 \pm 0.9) \times 10^{-3}$ [38], that its contribution can be safely neglected.

4 Signal yield determination

The yields of the $B^+ \to J/\psi K^+$, $B^0 \to J/\psi K^0_\text{S}$ and $\Lambda_b^0 \to J/\psi\Lambda$ decays are determined in bins of b-hadron p_T by performing extended unbinned maximum-likelihood fits to the reconstructed $J/\psi K^+$, $J/\psi K^0_\text{S}$ and $J/\psi\Lambda$ mass distributions, respectively. The fits are performed using the RooFit software package [39]. The mass distributions for the different p_T bins are shown in figures 5–9 in the appendix. The distributions obtained by combining the p_T bins are shown in figure 1. The B^0 and Λ_b^0 decay samples are fit simultaneously to take into account cross-feed from $B^0 \to J/\psi K^0_\text{S}$ decays reconstructed in the $\Lambda_b^0 \to J/\psi\Lambda$ sample and vice versa. The long and downstream samples are included separately in the simultaneous fit.

In the fits, the B^+, B^0 and Λ_b^0 signals are described using Hypatia functions [40] with tail parameters fixed from simulation. The peak positions and widths of the functions are allowed to vary in the fits to data separately in each bin of the b-hadron p_T. Combinatorial background is described using exponential functions. The cross-feed backgrounds from B^0 decays in the Λ_b^0 sample and Λ_b^0 decays in the B^0 sample are described using Johnson S_U distributions [41]. Their shape parameters are fixed from simulated $B^0 \to J/\psi K^0_\text{S}$ and $\Lambda_b^0 \to J/\psi\Lambda$ decays. The parameters of the signal and background shapes are allowed to differ between p_T bins and decay modes. The yield of the Λ_b^0 (B^0) cross-feed background in the B^0 (Λ_b^0) samples is

JHEP01(2026)159

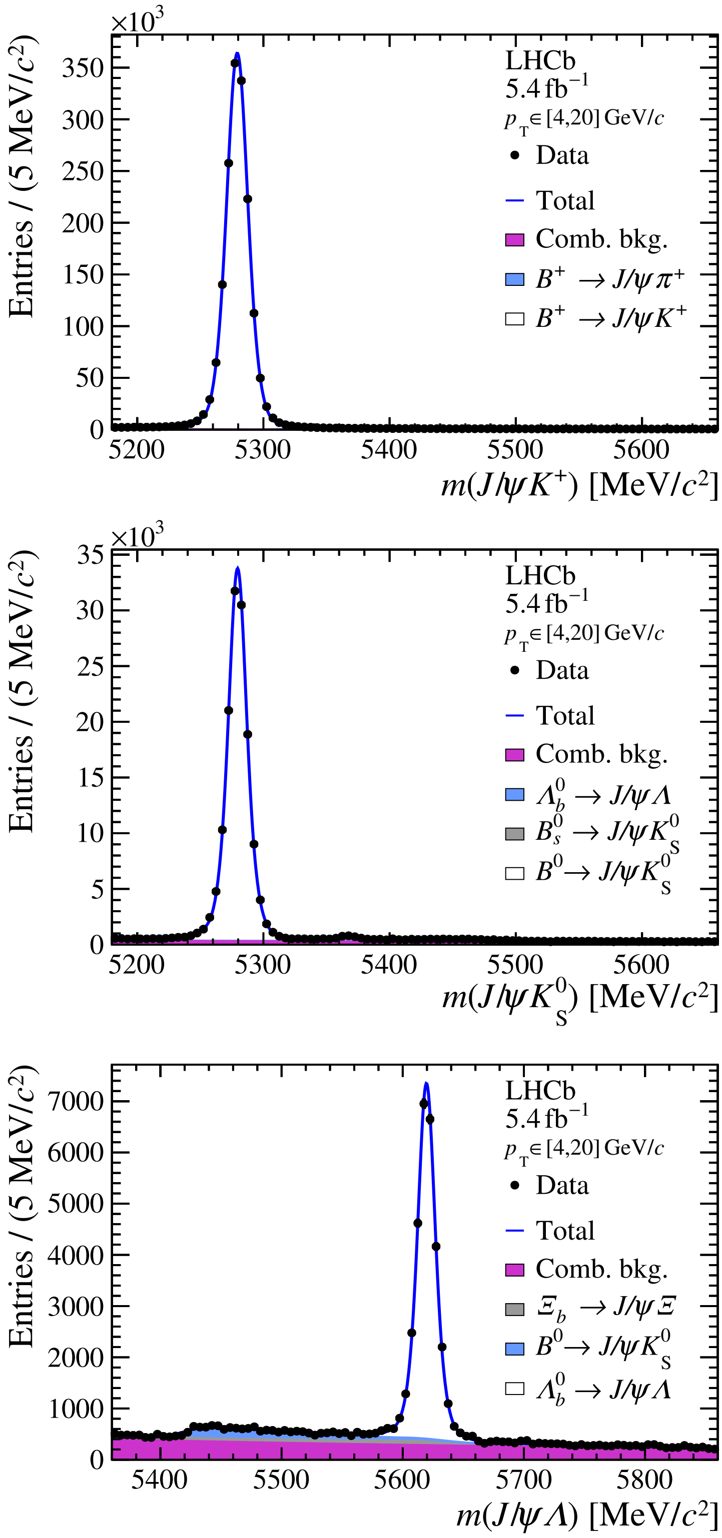

Figure 1. Mass distributions of selected (top) $J/\psi K^+$, (middle) $J/\psi K^0_S$ and (bottom) $J/\psi \Lambda$ candidates obtained by combining the data in the p_T range [4, 20] GeV/c. The line and shaded regions indicate the result of the fits and are obtained by summing the results of the fits to the individual p_T bins.

constrained from the corresponding yield of Λ_b^0 (B^0) decays in the Λ_b^0 (B^0) samples and the efficiency to correctly/incorrectly reconstruct the Λ_b^0 (B^0) candidates from simulation.

The background from $B^+ \to J/\psi\pi^+$ decays in the B^+ sample is described by a Gaussian function with power-law substituted tails on the left- and right-hand side of the distribution [42], with shape parameters fixed from simulated $B^+ \to J/\psi\pi^+$ decays. The yield of this background is constrained by the yield of the B^+ signal, the known branching-fraction ratio $\mathcal{B}(B^+ \to J/\psi\pi^+)/\mathcal{B}(B^+ \to J/\psi K^+)$ [35], and the relative efficiency to reconstruct and select $B^+ \to J/\psi\pi^+$ and $B^+ \to J/\psi K^+$ decays in simulation.

The background from $B_s^0 \to J/\psi K_S^0$ in the B^0 sample is modelled using the same Hypatia function describing the B^0 signal, but with a peak position shifted by the known B_s^0–B^0 mass difference of $87.37\,\mathrm{MeV}/c^2$ [35]. The yield of this background is constrained relative to that of the B^0 signal using the branching-fraction ratio $\mathcal{B}(B_s^0 \to J/\psi K_S^0)/\mathcal{B}(B^0 \to J/\psi K_S^0)$ from ref. [43], the production fraction ratio $f(b \to B_s^0)/f(b \to B^0)$ from ref. [15] and the relative efficiency to reconstruct and select B_s^0 and B^0 decays. The latter is determined from simulation.

The background from $\Xi_b{}^{+,0} \to J/\psi\Xi^{+,0}$ decays in the Λ_b^0 sample is described by a Johnson S_U distribution with parameters determined from simulation. Due to the long lifetime of the Ξ^- and Ξ^0 baryons, the contribution of these backgrounds to the long-track samples is very small and is neglected. The contribution in the downstream-track sample is also suppressed by the long lifetime. The yield of $\Xi_b{}^{+,0} \to J/\psi\Xi^{+,0}$ decays is expected to be $\mathcal{O}(1\%)$ of that of the $\Lambda_b^0 \to J/\psi\Lambda$ signal based on ref. [38], and is allowed to vary freely in the fit.

5 Branching fraction and isospin asymmetry determination

The ratio of the yields of the $\Lambda_b^0 \to J/\psi\Lambda$ and $B^0 \to J/\psi K_S^0$ decays in a b-hadron p_T interval can be expressed in terms of branching fractions and production fractions as

$$\frac{N[\Lambda_b^0]}{N[B^0]} = \frac{f(b \to \Lambda_b^0)}{f(b \to B^0)} \frac{\mathcal{B}(\Lambda_b^0 \to J/\psi\Lambda)}{\mathcal{B}(B^0 \to J/\psi K_S^0)} \frac{\mathcal{B}(\Lambda \to p\pi^-)}{\mathcal{B}(K_S^0 \to \pi^+\pi^-)} \frac{\epsilon[\Lambda_b^0]}{\epsilon[B^0]}\,. \tag{5.1}$$

Here, ϵ is the efficiency to reconstruct and select the given decay determined from simulation. The efficiencies are p_T-dependent mainly due to the long lifetimes of the Λ and K_S^0 hadrons, and a correlation between the b-hadron p_T and the typical boost of final-state particles along the beam axis. The ratio $\epsilon[\Lambda_b^0]/\epsilon[B^0]$ is less p_T dependent and is shown separately for the long and downstream categories in figure 2.

The known values of the K_S^0 and Λ branching fractions are $\mathcal{B}(K_S^0 \to \pi^+\pi^-) = 0.6920 \pm 0.0005$ and $\mathcal{B}(\Lambda \to p\pi^-) = 0.641 \pm 0.005$ [35], respectively. The production fraction of Λ_b^0 baryons in pp collisions has previously been studied by the LHCb collaboration at $\sqrt{s} = 13\,\mathrm{TeV}$ using semileptonic decays in ref. [15]. The ratio of $f(b \to \Lambda_b^0)$ and the sum of $f(b \to B^0)$ and $f(b \to B^+)$ is well described by the function $r(p_T) = A(p_1 + \exp(p_2 + p_3 \cdot p_T))$, with $A = 1.000 \pm 0.061$, $p_1 = (7.93 \pm 1.41) \times 10^{-2}$, $p_2 = -1.022 \pm 0.047$ and $p_3 = -0.107 \pm 0.002\,\mathrm{GeV}^{-1}c$. The ratio does not show any significant dependence on pseudorapidity [15]. Assuming isospin symmetry in high-energy pp collisions, $f(b \to \Lambda_b^0)/f(b \to B^0)$ is twice the value given by this function.

The $\Lambda_b^0 \to J/\psi\Lambda$ branching fraction is determined by fitting the ratio of the Λ_b^0 and B^0 yields as a function of p_T simultaneously between the long and downstream categories. In this

JHEP01(2026)159

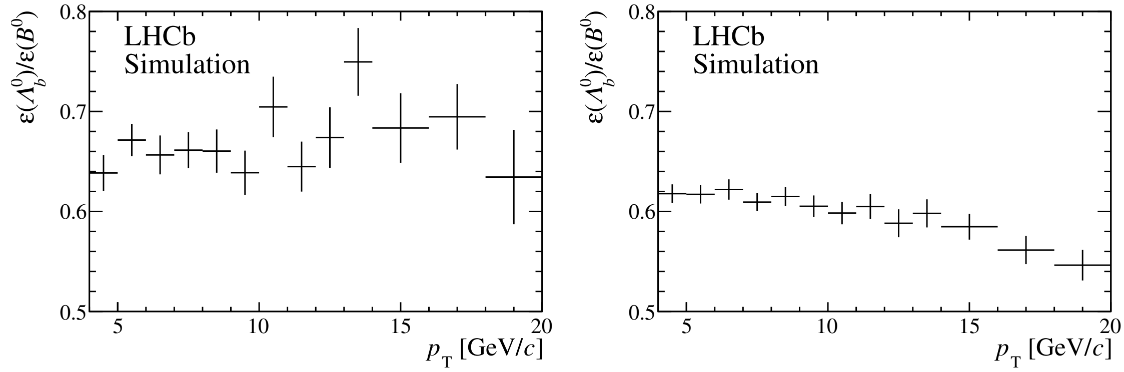

Figure 2. Efficiency ratio between $\Lambda_b^0 \to J/\psi \Lambda$ and $B^0 \to J/\psi K^0_S$ decays determined from corrected simulation samples in intervals of b-hadron transverse momentum for the (left) long-track and (right) downstream-track samples.

fit, the efficiency ratio, the parameter A, and the external branching fractions of the Λ and K^0_S decays are allowed to vary around their measured values with their uncertainties as a Gaussian prior, while the parameters p_1, p_2 and p_3 of $r(p_T)$ are constrained according to the covariance matrix reported in ref. [15]. The analysis is validated using pseudoexperiments generated with yields that are Poisson distributed as appropriate for the respective dataset. The pseudoexperiments are found to provide an unbiased estimate of the ratio of the $\Lambda_b^0 \to J/\psi \Lambda$ and $B^0 \to J/\psi K^0_S$ branching fractions. The isospin asymmetry is determined in bins of p_T from the efficiency-corrected yields of the $B^+ \to J/\psi K^+$ and $B^0 \to J/\psi K^0_S$ decays in data.

6 Systematic uncertainties

The analysis procedure is designed to minimise sources of systematic uncertainty in the measurement of $\mathcal{B}(\Lambda_b^0 \to J/\psi \Lambda)/\mathcal{B}(B^0 \to J/\psi K^0_S)$. The dominant sources of uncertainty on the measurement arise from the knowledge of $f(b \to \Lambda_b^0)/f(b \to B^0)$. A systematic uncertainty is also assigned on the external measurements of the $K^0_S \to \pi^+\pi^-$ and $\Lambda \to p\pi^-$ branching fractions. The estimated sources of systematic uncertainty on $\mathcal{B}(\Lambda_b^0 \to J/\psi \Lambda)/\mathcal{B}(B^0 \to J/\psi K^0_S)$ and A_I are summarised in table 1 and are described below. The statistical uncertainties on the branching fraction ratio and A_I measurements are determined by fixing all of the external parameters in the fit to their central values.

In the determination of the branching-fraction ratio from the yields of $\Lambda_b^0 \to J/\psi \Lambda$ and $B^0 \to J/\psi K^0_S$ decays, $f(b \to \Lambda_b^0)/f(b \to B^0)$ is evaluated at the bin centre of each b-hadron p_T bin. In reality there will be a distribution of candidates in p_T over the bin. Taking instead the value of $f(b \to \Lambda_b^0)/f(b \to B^0)$ one-third or two-thirds of the way across the bin changes the branching-fraction ratio by 1.4%.

Two sources of systematic uncertainty are related to the determination of the efficiencies from the simulation samples. The first of these is due to assumptions made in the matching of reconstructed candidates and true decays in the simulation, for which new efficiency values are derived from the simulated samples with a looser set of association criteria between detector energy deposits and the true particle trajectories. The second source of uncertainty is due to the finite size of the simulated samples, and is determined by comparing the baseline fit result to the one obtained fixing the efficiency ratio to its central value in the fit.

A systematic uncertainty is estimated on the choice of models used for determining the signal yields from data in section 4. The mass distributions are instead fit using a signal function with a Gaussian core and power-law substituted tails on the left- and right-hand side of the distribution. The difference in signal yields between the baseline fit results and those with the alternative fit functions is used to assign a systematic uncertainty.

Material interactions of $K^{\pm}$, K^0_S (K^0 and $\overline{K}^0$) and Λ hadrons in the detector could lead to a biased estimate of $\mathcal{B}(\Lambda_b^0 \to J/\psi\Lambda)/\mathcal{B}(B^0 \to J/\psi K^0_S)$, or A_I, if the detector material or hadronic cross-sections are not correctly described by simulation. For reference, in simulation 3% (3%) of K^0_S (Λ) hadrons interact before they could decay in the long sample and 5% (9%) before they could decay in the downstream sample. The most relevant material interactions happen in the vertex detector and in RICH 1. The amount of material in the vertex detector is known at the level of $\pm 6\%$ [44, 45]. The material in RICH 1 is well described by the simulation. Dedicated studies are performed using simulated samples of kaons and Λ baryons, comparing the results of the GEANT4 toolkit [31] to measurements of hadronic cross-sections on various materials reported in ref. [35]. To assess a systematic uncertainty, the survival probabilities of different particles are determined in the simulation when varying the amount of material in the vertex detector and when varying the hadronic cross-sections between different models in the GEANT4 toolkit.

The $\mathcal{B}(\Lambda_b^0 \to J/\psi\Lambda)/\mathcal{B}(B^0 \to J/\psi K^0_S)$ and A_I measurements are determined with a simultaneous fit that includes long and downstream samples. The ratio of Λ_b^0 and B^0 yields as a function of p_T is found to be in good agreement between the two samples (see section 7). Comparing the efficiency-corrected yields of the individual decays between the long and downstream samples, the yields of $\Lambda_b^0 \to J/\psi\Lambda$ decays are compatible, but the yields of $B^0 \to J/\psi K^0_S$ decays differ by 3.6%. Half of the difference on the values of $\mathcal{B}(\Lambda_b^0 \to J/\psi\Lambda)/\mathcal{B}(B^0 \to J/\psi K^0_S)$ obtained separately from the long and downstream samples is assigned as a systematic uncertainty. The same approach is used to assign a systematic uncertainty on A_I.

Systematic uncertainties are estimated for the corrections applied to simulation to reproduce the data, namely due to the finite size of various calibration samples, and the choice of binning used for determining the corrections. For the measurement of $\mathcal{B}(\Lambda_b^0 \to J/\psi\Lambda)/\mathcal{B}(B^0 \to J/\psi K^0_S)$, these systematic uncertainties are completely dominated by corrections on the production kinematics of the b hadrons. For the measurement of A_I, the systematic uncertainties due to the corrections applied to simulation are negligible because it is assumed that B^0 and B^+ mesons have the same kinematic distributions. However, additional sources of systematic uncertainty arise due to the need to reconstruct an additional track for the $B^0 \to J/\psi K^0_S$ decay and the use of particle-identification requirements to select the K^+ meson. They are determined taking into account the individual contributions to differences in track reconstruction efficiency between data and simulation. The efficiency for a kaon to satisfy the particle-identification requirements used in the reconstruction of B^+ candidates is determined from data using samples of $D^{*+} \to D^0\pi^+$ decays, with $D^0 \to K^-\pi^+$, as a function of the kaon momentum and the multiplicity of charged particles in the event [46]. The measurement of A_I is also sensitive to the knowledge of the lifetime ratio τ_{B^+}/τ_{B^0}, which is taken from ref. [17].

JHEP01(2026)159

Source	$\frac{\mathcal{B}(\Lambda_b^0 \to J/\psi\Lambda)}{\mathcal{B}(B^0 \to J/\psi K_S^0)}$ [%]	A_I [$\times 10^{-2}$]
$f(b \to \Lambda_b^0)/f(b \to B^0)$	8.27	–
K_S^0 and Λ branching fractions	0.78	0.01
$f(b \to \Lambda_b^0)/f(b \to B^0)$ p_T-binning	1.40	–
Truth matching	1.40	0.60
Simulation sample sizes	1.20	0.04
Mass line shapes	0.10	0.10
Material interactions	0.50	0.35
Long/downstream compatibility	1.80	0.85
Data-simulation corrections	0.60	–
Pion track reconstruction efficiency	–	0.50
Kaon particle identification	–	0.50
b-hadron lifetimes	–	0.18

Table 1. Summary of sources of relative systematic uncertainty on the $\mathcal{B}(\Lambda_b^0 \to J/\psi\Lambda)/\mathcal{B}(B^0 \to J/\psi K_S^0)$ measurement and absolute systematic uncertainty on the A_I measurement. All uncertainties are treated as uncorrelated.

7 Results

Figure 3 shows the measured isospin asymmetry between B^0 and B^+ decays, in bins of the B-meson p_T, averaging the value of the $B^0 \to J/\psi K_S^0$ branching fraction between the long- and downstream-track categories. The measured asymmetry shows no significant p_T dependence and the two distributions are found to be compatible at the percent level. There is also no evidence for any significant deviation from the expectation that $A_I \approx 0$. An average value of A_I is obtained by performing a χ^2 fit to the measurements in intervals of p_T in the long- and downstream-track samples, under the assumption of isospin symmetry in the production of B^0 and B^+ mesons. The resulting value of A_I is

$$A_I = -0.0135 \pm 0.0004 \pm 0.0133\,,$$

where the first uncertainty is statistical and the second systematic. This A_I value is consistent with recent measurements of the same quantity by other experiments [5, 18]. Assuming instead isospin symmetry between decays, the ratio of production cross-sections of B^+ and B^0 mesons is determined to be

$$f(b \to B^+)/f(b \to B^0) = 1.027 \pm 0.001 \pm 0.027$$

where the first uncertainty is statistical and the second systematic.

Figure 4 shows the measured ratio between the yields of $\Lambda_b^0 \to J/\psi\Lambda$ and $B^0 \to J/\psi K_S^0$ decays in bins of p_T. The data for the long- and downstream-track samples provide consistent results considering the ratio of efficiencies to select and reconstruct Λ_b^0 and B^0 signal in those

JHEP01(2026)159

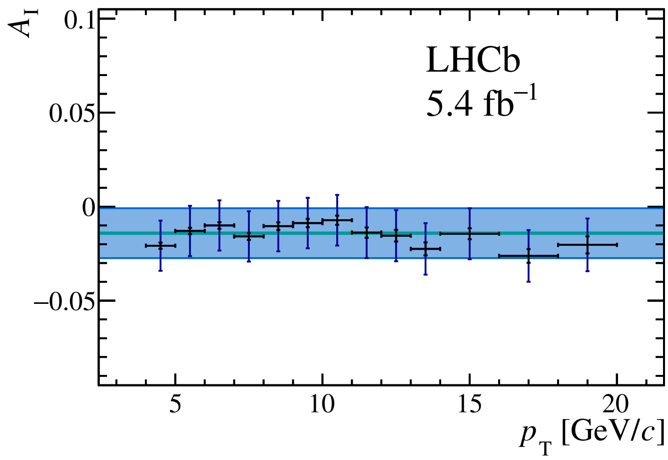

Figure 3. Isospin asymmetry between $B^0 \to J/\psi K^0$ and $B^+ \to J/\psi K^+$ decays in bins of B-meson p_{T} for the long and downstream-track samples averaged. The inner (outer) bars indicate the statistical (total) uncertainty on the data points. The green (blue) band indicates the average isospin asymmetry across the p_{T} bins and its statistical (total) uncertainty.

categories. The fit to the ratio of yields in bins of p_{T} gives

$$\frac{\mathcal{B}(\Lambda_b^0 \to J/\psi \Lambda)}{\mathcal{B}(B^0 \to J/\psi K_{\mathrm{S}}^0)} = 0.750 \pm 0.005 \pm 0.022 \pm 0.005 \pm 0.062\,,$$

where the first uncertainty is statistical, the second systematic, the third due to external inputs on $\mathcal{B}(K_{\mathrm{S}}^0 \to \pi^+\pi^-)$ and $\mathcal{B}(\Lambda \to p\pi^-)$ and the fourth due to $f(b \to \Lambda_b^0)/f(b \to B^0)$. The fit has a χ^2 of 23.9 with 25 degrees of freedom.

Using the world average value of $\mathcal{B}(B^0 \to J/\psi K_{\mathrm{S}}^0) = (4.45 \pm 0.11) \times 10^{-4}$ from ref. [35], the branching fraction is determined to be

$$\mathcal{B}(\Lambda_b^0 \to J/\psi \Lambda) = (3.34 \pm 0.02 \pm 0.10 \pm 0.08 \pm 0.28) \times 10^{-4}\,,$$

where the third uncertainty also includes the uncertainty on $\mathcal{B}(B^0 \to J/\psi K_{\mathrm{S}}^0)$. Note that the value used for $\mathcal{B}(B^0 \to J/\psi K_{\mathrm{S}}^0)$ averages measurements with slightly different assumptions on the relative production of $B^0\overline{B}^0$ and B^+B^- mesons in $\Upsilon(4S)$ decays. However, a reinterpretation of older measurements of the branching fraction, taking possible production asymmetries into account, gives a very consistent value [19].

8 Summary

A measurement of the branching-fraction ratio between $\Lambda_b^0 \to J/\psi \Lambda$ and $B^0 \to J/\psi K_{\mathrm{S}}^0$ decays has been performed. The measurement uses a dataset corresponding to an integrated luminosity of 5.4 fb^{-1} collected in proton-proton collisions at $\sqrt{s} = 13$ TeV by the LHCb experiment. The ratio $\mathcal{B}(\Lambda_b^0 \to J/\psi \Lambda)/\mathcal{B}(B^0 \to J/\psi K_{\mathrm{S}}^0)$ is found to be 0.750 ± 0.066, combining all sources of uncertainty in quadrature. This value can be compared to the ratio of lifetimes between Λ_b^0 baryons and B^0 mesons, $\tau_{\Lambda_b^0}/\tau_{B^0} = 0.964 \pm 0.007$ [17, 35]. Accounting for the 50% probability for a K^0 meson to produce a K_{S}^0, the partial width of the $\Lambda_b^0 \to J/\psi \Lambda$

JHEP01(2026)159

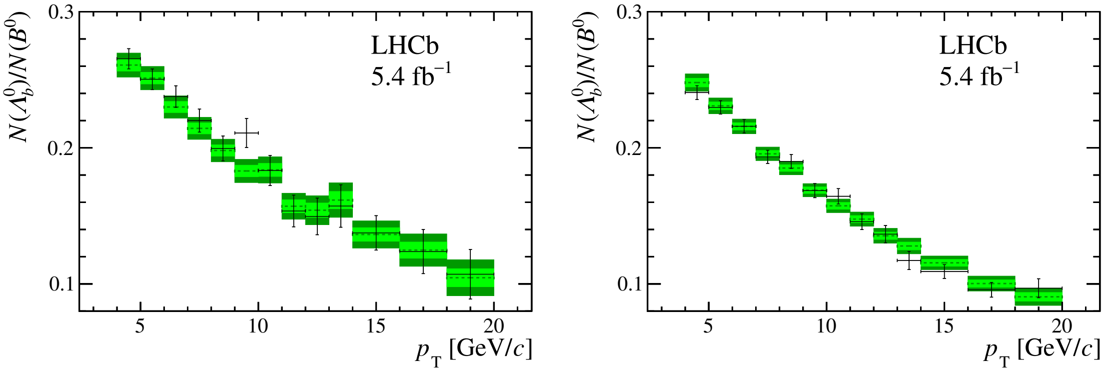

Figure 4. Ratio of yields between $\Lambda_b^0 \to J/\psi \Lambda$ and $B^0 \to J/\psi K_S^0$ decays in bins of b-hadron p_T for the (left) long-track and (right) downstream-track samples. The dashed line shows the result of the fit described in the text. The inner and outer shaded regions correspond to 68% and 95% confidence intervals, respectively. These regions include contributions from the statistical uncertainty on the event yields and uncertainties on the external parameters entering the branching-fraction ratio fit.

decay is found to be approximately 39% of that of the $B^0 \to J/\psi K^0$ decay. The resulting $\Lambda_b^0 \to J/\psi \Lambda$ branching fraction is compatible with estimates based on perturbative QCD and QCD factorisation approaches obtained in refs. [47] and [48], respectively. The partial widths of the $B^+ \to J/\psi K^+$ and $B^0 \to J/\psi K^0$ decays are compatible at the percent level.

Acknowledgments

We express our gratitude to our colleagues in the CERN accelerator departments for the excellent performance of the LHC. We thank the technical and administrative staff at the LHCb institutes. We acknowledge support from CERN and from the national agencies: ARC (Australia); CAPES, CNPq, FAPERJ and FINEP (Brazil); MOST and NSFC (China); CNRS/IN2P3 (France); BMBF, DFG and MPG (Germany); INFN (Italy); NWO (Netherlands); MNiSW and NCN (Poland); MCID/IFA (Romania); MICIU and AEI (Spain); SNSF and SER (Switzerland); NASU (Ukraine); STFC (United Kingdom); DOE NP and NSF (U.S.A.). We acknowledge the computing resources that are provided by ARDC (Australia), CBPF (Brazil), CERN, IHEP and LZU (China), IN2P3 (France), KIT and DESY (Germany), INFN (Italy), SURF (Netherlands), Polish WLCG (Poland), IFIN-HH (Romania), PIC (Spain), CSCS (Switzerland), and GridPP (United Kingdom). We are indebted to the communities behind the multiple open-source software packages on which we depend. Individual groups or members have received support from Key Research Program of Frontier Sciences of CAS, CAS PIFI, CAS CCEPP, Fundamental Research Funds for the Central Universities, and Sci. & Tech. Program of Guangzhou (China); Minciencias (Colombia); EPLANET, Marie Skłodowska-Curie Actions, ERC and NextGenerationEU (European Union); A*MIDEX, ANR, IPhU and Labex P2IO, and Région Auvergne-Rhône-Alpes (France); Alexander-von-Humboldt Foundation (Germany); ICSC (Italy); Severo Ochoa and María de Maeztu Units of Excellence, GVA, XuntaGal, GENCAT, InTalent-Inditex and Prog. Atracción Talento CM (Spain); SRC (Sweden); the Leverhulme Trust, the Royal Society and UKRI (United Kingdom).

JHEP01(2026)159

A Mass distributions of candidates in transverse-momentum bins

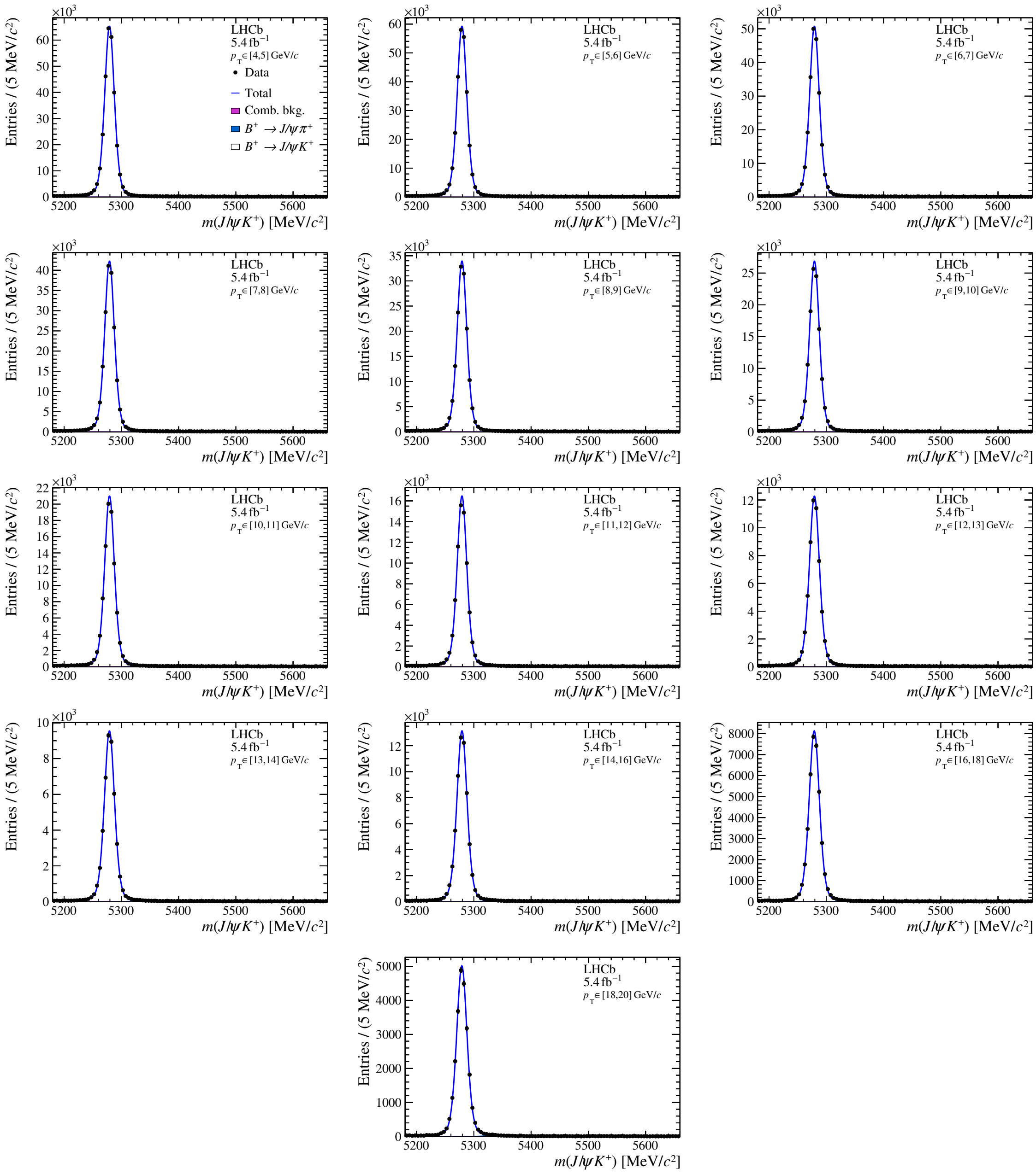

Figure 5. Reconstructed $J/\psi K^+$ mass distribution of selected $B^+ \to J/\psi K^+$ candidates in bins of B^+ meson p_{T}. The line and shaded regions show the result of the fit described in the text.

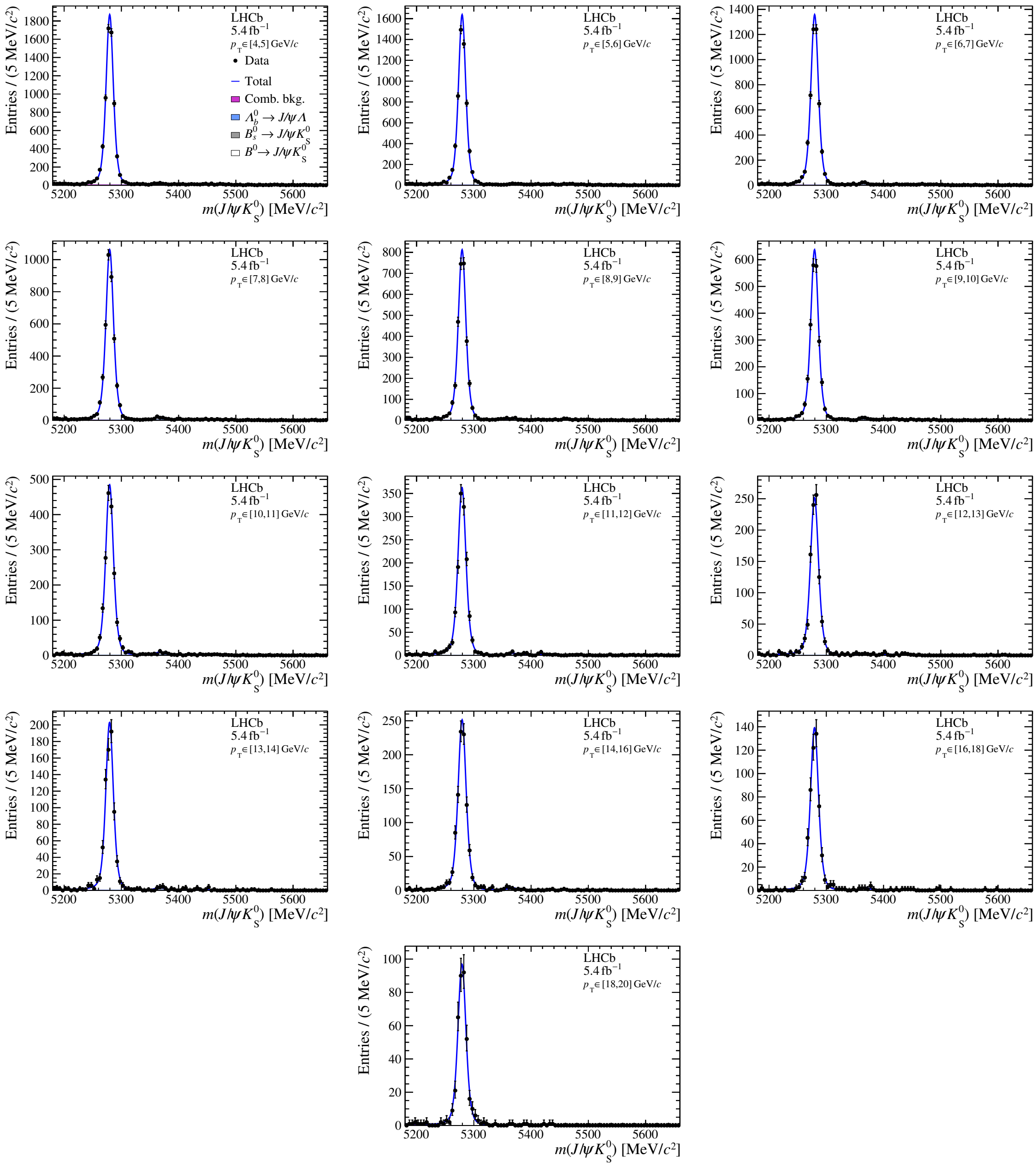

Figure 6. Reconstructed $J/\psi K^0_S$ mass distribution of selected $B^0 \to J/\psi K^0_S$ candidates in bins of B^0 meson p_T, reconstructed from long-category tracks. The line and shaded regions show the result of the fit described in the text.

JHEP01(2026)159

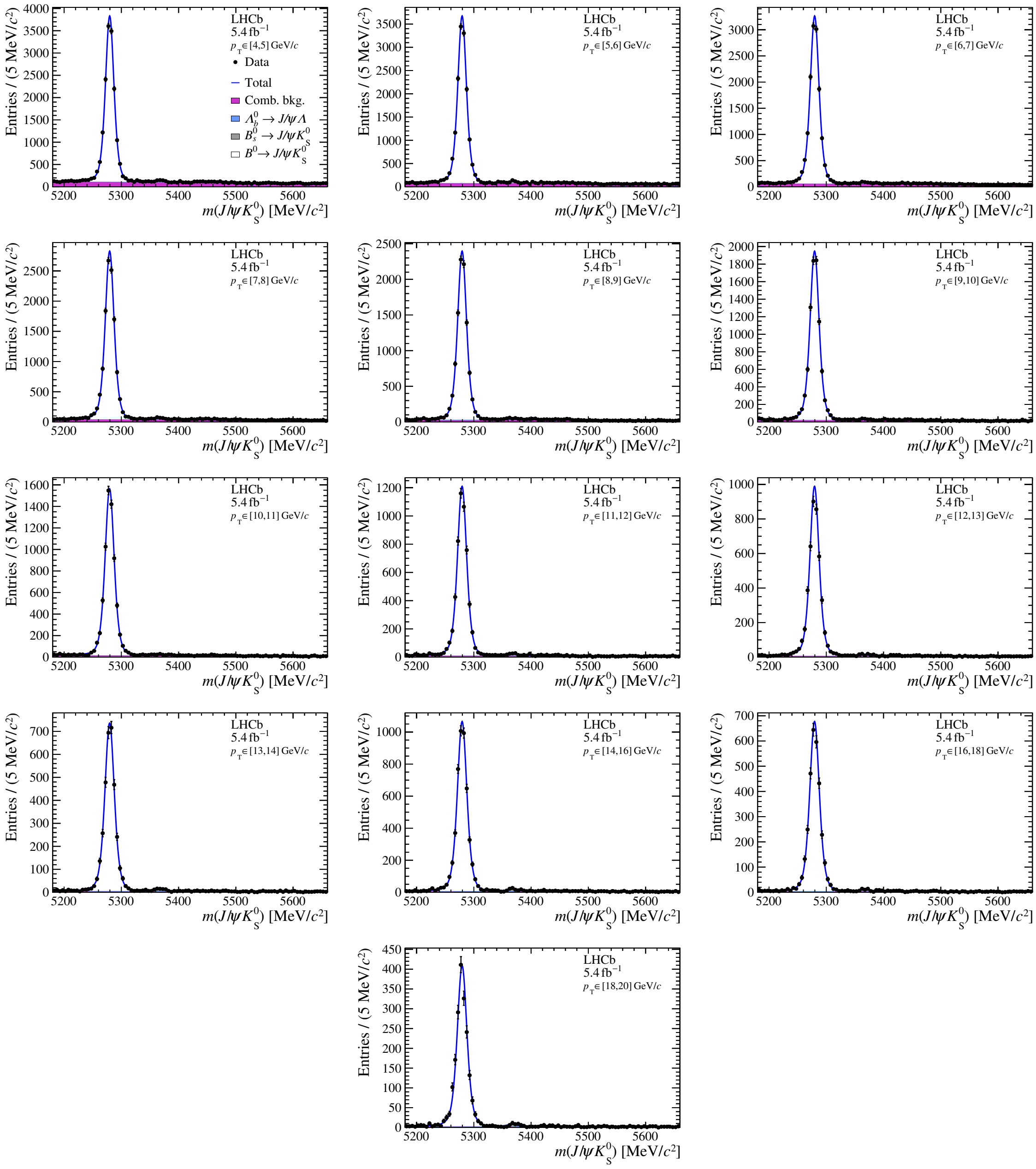

Figure 7. Reconstructed $J/\psi K^0_S$ mass distribution of selected $B^0 \to J/\psi K^0_S$ candidates in bins of B^0 meson p_T, reconstructed from downstream-category tracks. The line and shaded regions show the result of the fit described in the text.

JHEP01(2026)159

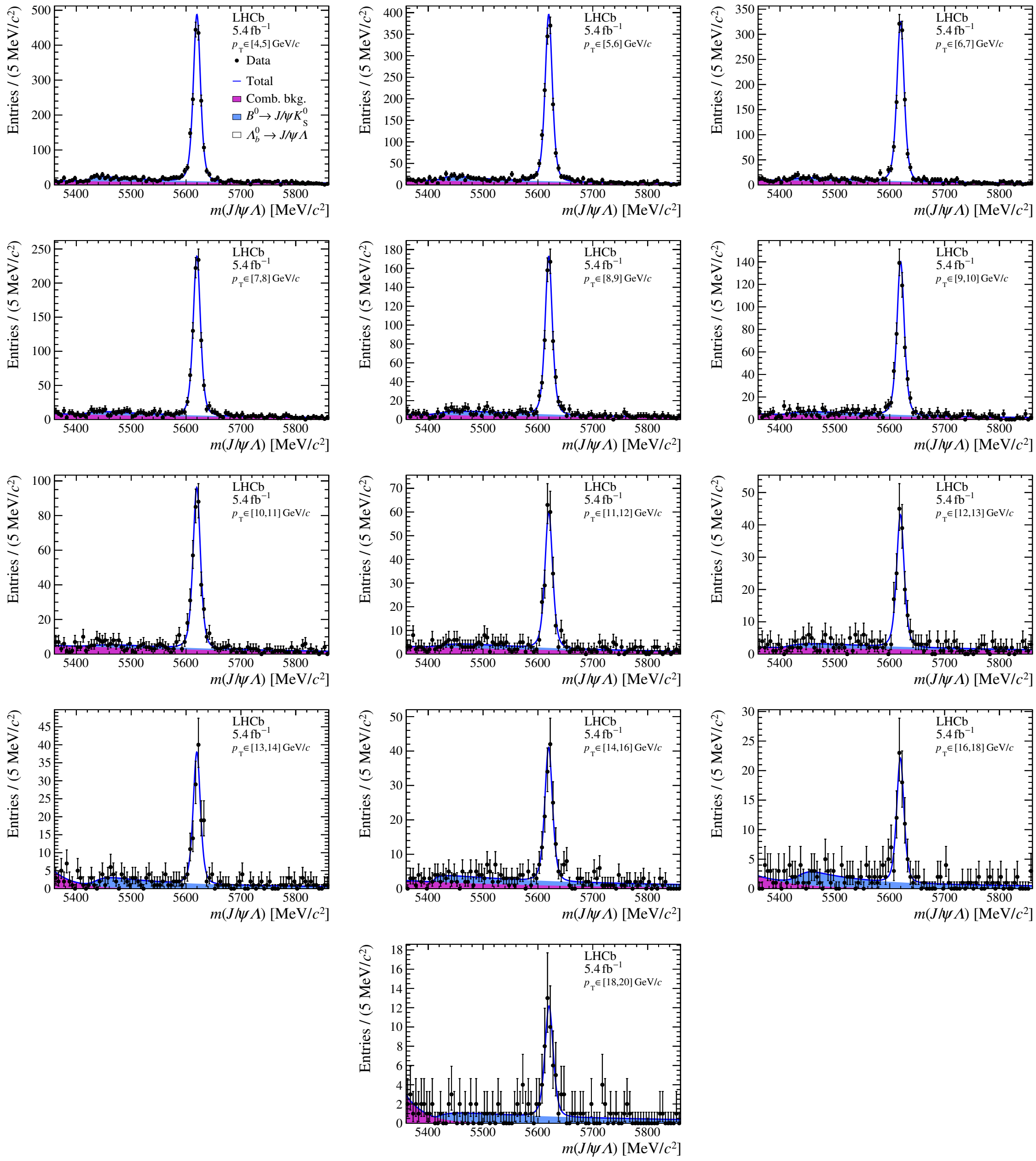

Figure 8. Reconstructed $J/\psi\Lambda$ mass distribution of selected $\Lambda_b^0 \to J/\psi\Lambda$ candidates in bins of Λ baryon $p_{\rm T}$, reconstructed from long-category tracks. The line and shaded regions show the result of the fit described in the text.

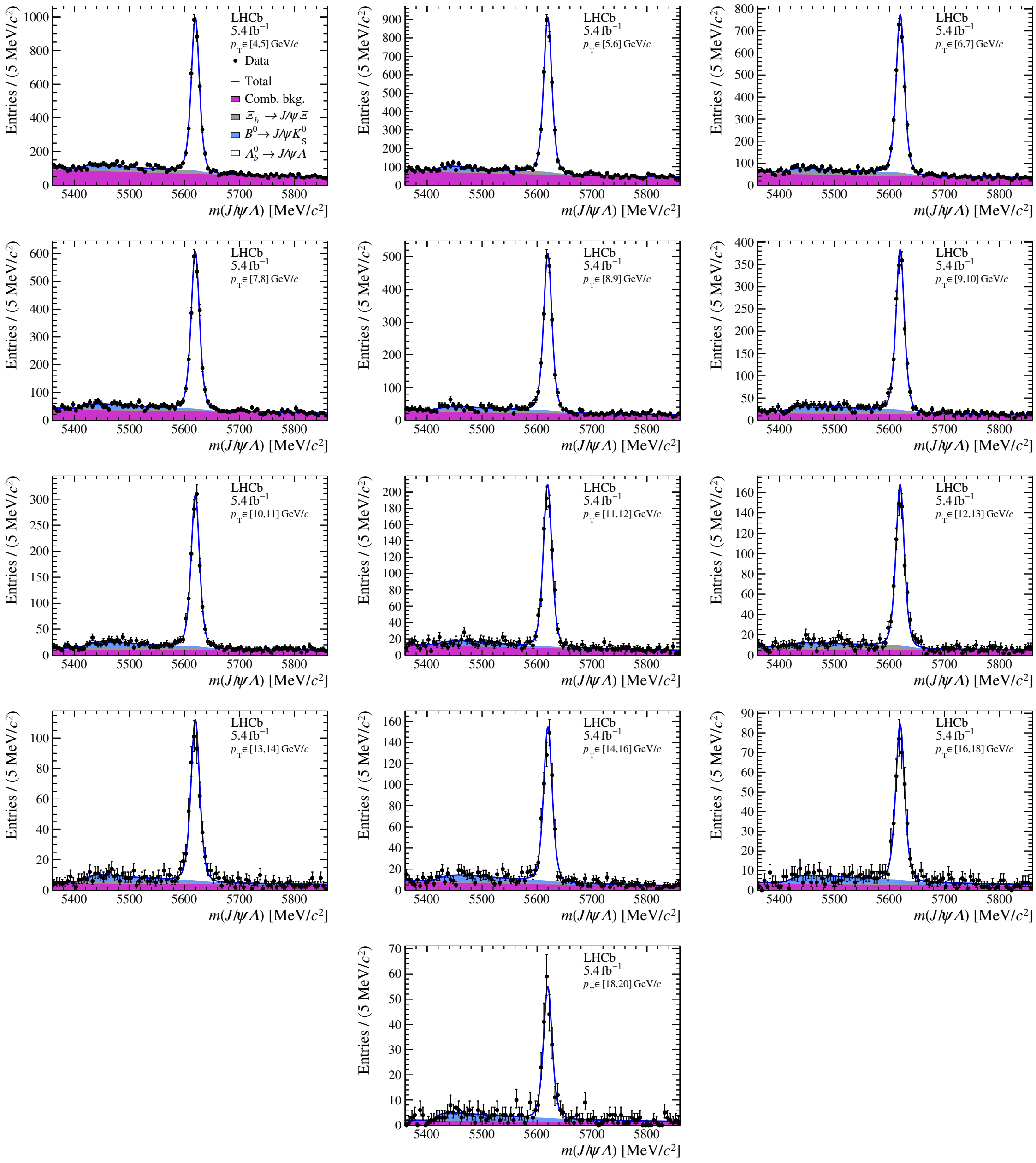

Figure 9. Reconstructed $J/\psi\Lambda$ mass distribution of selected $\Lambda_b^0 \to J/\psi\Lambda$ candidates in bins of Λ_b^0 baryon p_{T}, reconstructed from downstream-category tracks. The line and shaded regions show the result of the fit described in the text.

JHEP01(2026)159

Data Availability Statement. All LHCb scientific output is published in journals, with preliminary results made available in Conference Reports. All are Open Access, without restriction on use beyond the standard conditions agreed by CERN. Data associated to the plots in this publication as well as in supplementary materials are made available on the CERN document server at http://cdsweb.cern.ch/record/2942686. This information is taken from the LHCb External Data Access Policy which can be downloaded at http://opendata.cern.ch/record/410.

Code Availability Statement. This article has no associated code or the code will not be deposited.

References

[1] LHCb collaboration, *Analysis of Neutral B-Meson Decays into Two Muons*, *Phys. Rev. Lett.* **128** (2022) 041801 [arXiv:2108.09284] [INSPIRE].

[2] LHCb collaboration, *Measurement of the $B_s^0 \to \mu^+\mu^-$ decay properties and search for the $B^0 \to \mu^+\mu^-$ and $B_s^0 \to \mu^+\mu^-\gamma$ decays*, *Phys. Rev. D* **105** (2022) 012010 [arXiv:2108.09283] [INSPIRE].

[3] CMS collaboration, *Measurement of the $B_S^0 \to \mu^+\mu^-$ decay properties and search for the $B^0 \to \mu^+\mu^-$ decay in proton-proton collisions at $\sqrt{s} = 13$ TeV*, *Phys. Lett. B* **842** (2023) 137955 [arXiv:2212.10311] [INSPIRE].

[4] ATLAS collaboration, *Study of the rare decays of B_s^0 and B^0 mesons into muon pairs using data collected during 2015 and 2016 with the ATLAS detector*, *JHEP* **04** (2019) 098 [arXiv:1812.03017] [INSPIRE].

[5] BELLE collaboration, *Test of lepton flavor universality and search for lepton flavor violation in $B \to K\ell\ell$ decays*, *JHEP* **03** (2021) 105 [arXiv:1908.01848] [INSPIRE].

[6] BaBar collaboration, *Measurement of branching fractions and charge asymmetries for exclusive B decays to charmonium*, *Phys. Rev. Lett.* **94** (2005) 141801 [hep-ex/0412062] [INSPIRE].

[7] Belle collaboration, *Measurements of the absolute branching fractions of $B^+ \to X_{c\bar{c}}K^+$ and $B^+ \to \bar{D}^{(*)0}\pi^+$ at Belle*, *Phys. Rev. D* **97** (2018) 012005 [arXiv:1709.06108] [INSPIRE].

[8] Belle collaboration, *Evidence for $B^+ \to h_c K^+$ and observation of $\eta_c(2S) \to p\bar{p}\pi^+\pi^-$*, *Phys. Rev. D* **100** (2019) 012001 [arXiv:1903.06414] [INSPIRE].

[9] CLEO collaboration, *Measurement of the decay amplitudes and branching fractions of $b \to J/\psi K^*$ and $b \to J/\psi K$ decays*, *Phys. Rev. Lett.* **79** (1997) 4533 [hep-ex/9702013] [INSPIRE].

[10] CLEO collaboration, *Study of exclusive two-body B^0 meson decays to charmonium*, *Phys. Rev. D* **62** (2000) 051101 [hep-ex/0004032] [INSPIRE].

[11] D0 collaboration, *Measurement of the production fraction times branching fraction $f(b \to \Lambda_b) \cdot \mathcal{B}(\Lambda_b \to J/\psi\Lambda)$*, *Phys. Rev. D* **84** (2011) 031102 [arXiv:1105.0690] [INSPIRE].

JHEP01(2026)159

[12] CDF collaboration, *Observation of $\Lambda_b^0 \to J/\psi\Lambda$ at the Fermilab proton antiproton collider*, Phys. Rev. D **55** (1997) 1142 [INSPIRE].

[13] T. Blake, S. Meinel and D. van Dyk, *Bayesian Analysis of $b \to s\mu^+\mu^-$ Wilson Coefficients using the Full Angular Distribution of $\Lambda_b \to \Lambda(\to p\pi^-)\mu^+\mu^-$ Decays*, Phys. Rev. D **101** (2020) 035023 [arXiv:1912.05811] [INSPIRE].

[14] LHCb collaboration, *Measurement of b-hadron production fractions in 7 TeV pp collisions*, Phys. Rev. D **85** (2012) 032008 [arXiv:1111.2357] [INSPIRE].

[15] LHCb collaboration, *Measurement of b hadron fractions in 13 TeV pp collisions*, Phys. Rev. D **100** (2019) 031102(R) [arXiv:1902.06794] [INSPIRE].

[16] J. Lyon and R. Zwicky, *Isospin asymmetries in $B \to (K^*, \rho)\gamma/l^+l^-$ and $B \to Kl^+l^-$ in and beyond the standard model*, Phys. Rev. D **88** (2013) 094004 [arXiv:1305.4797] [INSPIRE].

[17] Heavy Flavor Averaging Group collaboration, *Averages of b-hadron, c-hadron, and τ-lepton properties as of 2021*, Phys. Rev. D **107** (2023) 052008 [arXiv:2206.07501] [INSPIRE].

[18] Belle II collaboration, *Measurements of the branching fraction, isospin asymmetry, and lepton-universality ratio in $B \to J/\psi K$ decays at Belle II*, arXiv:2207.11275 [INSPIRE].

[19] M. Jung, *Branching ratio measurements and isospin violation in B-meson decays*, Phys. Lett. B **753** (2016) 187 [arXiv:1510.03423] [INSPIRE].

[20] W. Fetscher et al., *Regeneration of arbitrary coherent neutral kaon states: A new method for measuring the $K^0 - \bar{K}^0$ forward scattering amplitude*, Z. Phys. C **72** (1996) 543 [INSPIRE].

[21] LHCb collaboration, *The LHCb Detector at the LHC*, 2008 *JINST* **3** S08005 [INSPIRE].

[22] LHCb collaboration, *LHCb Detector Performance*, Int. J. Mod. Phys. A **30** (2015) 1530022 [arXiv:1412.6352] [INSPIRE].

[23] R. Aaij et al., *The LHCb Trigger and its Performance in 2011*, 2013 *JINST* **8** P04022 [arXiv:1211.3055] [INSPIRE].

[24] R. Aaij et al., *Design and performance of the LHCb trigger and full real-time reconstruction in Run 2 of the LHC*, 2019 *JINST* **14** P04013 [arXiv:1812.10790] [INSPIRE].

[25] N.A. Grieser et al., *The LHCb Stripping Project: Sustainable Legacy Data Processing for High-Energy Physics*, Comput. Softw. Big Sci. **9** (2025) 21 [arXiv:2509.05294] [INSPIRE].

[26] T. Sjöstrand, S. Mrenna and P. Skands, *A Brief Introduction to PYTHIA 8.1*, Comput. Phys. Commun. **178** (2008) 852 [arXiv:0710.3820] [INSPIRE].

[27] T. Sjöstrand, S. Mrenna and P. Skands, *PYTHIA 6.4 Physics and Manual*, JHEP **05** (2006) 026 [hep-ph/0603175] [INSPIRE].

[28] I. Belyaev et al., *Handling of the generation of primary events in Gauss, the LHCb simulation framework*, J. Phys. Conf. Ser. **331** (2011) 032047 [INSPIRE].

[29] D.J. Lange, *The EvtGen particle decay simulation package*, Nucl. Instrum. Meth. A **462** (2001) 152 [INSPIRE].

[30] N. Davidson, T. Przedzinski and Z. Was, *PHOTOS interface in C++: Technical and Physics Documentation*, Comput. Phys. Commun. **199** (2016) 86 [arXiv:1011.0937] [INSPIRE].

[31] J. Allison et al., *Geant4 developments and applications*, IEEE Trans. Nucl. Sci. **53** (2006) 270 [INSPIRE].

[32] Geant4 collaboration, *GEANT4 — A Simulation Toolkit*, Nucl. Instrum. Meth. A **506** (2003) 250 [INSPIRE].

[33] M. Clemencic et al., *The LHCb simulation application, Gauss: Design, evolution and experience*, *J. Phys. Conf. Ser.* **331** (2011) 032023 [INSPIRE].

[34] LHCb collaboration, *Measurement of the $\Lambda_b^0 \to J/\psi\Lambda$ angular distribution and the Λ_b^0 polarisation in pp collisions*, *JHEP* **06** (2020) 110 [arXiv:2004.10563] [INSPIRE].

[35] Particle Data Group collaboration, *Review of particle physics*, *Phys. Rev. D* **110** (2024) 030001 [INSPIRE].

[36] W.D. Hulsbergen, *Decay chain fitting with a Kalman filter*, *Nucl. Instrum. Meth. A* **552** (2005) 566 [physics/0503191] [INSPIRE].

[37] T. Chen and C. Guestrin, *XGBoost: A Scalable Tree Boosting System*, arXiv:1603.02754 [DOI:10.1145/2939672.2939785] [INSPIRE].

[38] LHCb collaboration, *Isospin amplitudes in $\Lambda_b^0 \to J/\psi\Lambda(\Sigma^0)$ and $\Xi_b^0 \to J/\psi\Xi^0(\Lambda)$ decays*, *Phys. Rev. Lett.* **124** (2020) 111802 [arXiv:1912.02110] [INSPIRE].

[39] W. Verkerke and D.P. Kirkby, *The RooFit toolkit for data modeling*, *eConf C* **0303241** (2003) MOLT007 [physics/0306116] [INSPIRE].

[40] D. Martínez Santos and F. Dupertuis, *Mass distributions marginalized over per-event errors*, *Nucl. Instrum. Meth. A* **764** (2014) 150 [arXiv:1312.5000] [INSPIRE].

[41] N.L. Johnson, *Systems of frequency curves generated by methods of translation*, *Biometrika* **36** (1949) 149 [INSPIRE].

[42] T. Skwarnicki, *A study of the radiative CASCADE transitions between the Upsilon-Prime and Upsilon resonances*, Ph.D. Thesis, Institute of Nuclear Physics, Krakow, Poland (1986) [INSPIRE].

[43] LHCb collaboration, *Measurement of the time-dependent CP asymmetries in $B_s^0 \to J/\psi K_S^0$*, *JHEP* **06** (2015) 131 [arXiv:1503.07055] [INSPIRE].

[44] M. Alexander et al., *Mapping the material in the LHCb vertex locator using secondary hadronic interactions*, 2018 *JINST* **13** P06008 [arXiv:1803.07466] [INSPIRE].

[45] R. Aaij et al., *Performance of the LHCb Vertex Locator*, 2014 *JINST* **9** P09007 [arXiv:1405.7808] [INSPIRE].

[46] R. Aaij et al., *Selection and processing of calibration samples to measure the particle identification performance of the LHCb experiment in Run 2*, *Eur. Phys. J. Tech. Instrum.* **6** (2019) 1 [arXiv:1803.00824] [INSPIRE].

[47] Z. Rui and Z.-T. Zou, *Charmonium decays of beauty baryons in the perturbative QCD approach*, *Phys. Rev. D* **109** (2024) 033013 [arXiv:2310.19031] [INSPIRE].

[48] Y.-K. Hsiao and C.-C. Lih, *Fragmentation fraction f_{Ω_b} and the $\Omega_b \to \Omega J/\psi$ decay in the light-front formalism*, *Phys. Rev. D* **105** (2022) 056015 [arXiv:2110.00945] [INSPIRE].

JHEP01(2026)159

The LHCb collaboration

R. Aaij[38], A.S.W. Abdelmotteleb[57], C. Abellan Beteta[51], F. Abudinén[57], T. Ackernley[61], A.A. Adefisoye[69], B. Adeva[47], M. Adinolfi[55], P. Adlarson[85], C. Agapopoulou[14], C.A. Aidala[87], Z. Ajaltouni[11], S. Akar[11], K. Akiba[38], M. Akthar[40], P. Albicocco[28], J. Albrecht[19,g], R. Aleksiejunas[80], F. Alessio[49], P. Alvarez Cartelle[56], R. Amalric[16], S. Amato[3], J.L. Amey[55], Y. Amhis[14], L. An[6], L. Anderlini[27], M. Andersson[51], P. Andreola[51], M. Andreotti[26], S. Andres Estrada[84], A. Anelli[31,p,49], D. Ao[7], C. Arata[12], F. Archilli[37,w], Z. Areg[69], M. Argenton[26], S. Arguedas Cuendis[9,49], L. Arnone[31,p], A. Artamonov[44], M. Artuso[69], E. Aslanides[13], R. Ataíde Da Silva[50], M. Atzeni[65], B. Audurier[12], J.A. Authier[15], D. Bacher[64], I. Bachiller Perea[50], S. Bachmann[22], M. Bachmayer[50], J.J. Back[57], P. Baladron Rodriguez[47], V. Balagura[15], A. Balboni[26], W. Baldini[26], Z. Baldwin[78], L. Balzani[19], H. Bao[7], J. Baptista de Souza Leite[2], C. Barbero Pretel[47,12], M. Barbetti[27], I.R. Barbosa[70], R.J. Barlow[63], M. Barnyakov[25], S. Barsuk[14], W. Barter[59], J. Bartz[69], S. Bashir[40], B. Batsukh[5], P.B. Battista[14], A. Bay[50], A. Beck[65], M. Becker[19], F. Bedeschi[35], I.B. Bediaga[2], N.A. Behling[19], S. Belin[47], A. Bellavista[25], K. Belous[44], I. Belov[29], I. Belyaev[36], G. Benane[13], G. Bencivenni[28], E. Ben-Haim[16], A. Berezhnoy[44], R. Bernet[51], S. Bernet Andres[46], A. Bertolin[33], C. Betancourt[51], F. Betti[59], J. Bex[56], Ia. Bezshyiko[51], O. Bezshyyko[86], J. Bhom[41], M.S. Bieker[18], N.V. Biesuz[26], A. Biolchini[38], M. Birch[62], F.C.R. Bishop[10], A. Bitadze[63], A. Bizzeti[27,q], T. Blake[57,c], F. Blanc[50], J.E. Blank[19], S. Blusk[69], V. Bocharnikov[44], J.A. Boelhauve[19], O. Boente Garcia[15], T. Boettcher[68], A. Bohare[59], A. Boldyrev[44], C.S. Bolognani[82], R. Bolzonella[26,m], R.B. Bonacci[1], N. Bondar[44,49], A. Bordelius[49], F. Borgato[33,49], S. Borghi[63], M. Borsato[31,p], J.T. Borsuk[83], E. Bottalico[61], S.A. Bouchiba[50], M. Bovill[64], T.J.V. Bowcock[61], A. Boyer[49], C. Bozzi[26], J.D. Brandenburg[88], A. Brea Rodriguez[50], N. Breer[19], J. Brodzicka[41], A. Brossa Gonzalo[47,†], J. Brown[61], D. Brundu[32], E. Buchanan[59], M. Burgos Marcos[82], A.T. Burke[63], C. Burr[49], C. Buti[27], J.S. Butter[56], J. Buytaert[49], W. Byczynski[49], S. Cadeddu[32], H. Cai[75], Y. Cai[5], A. Caillet[16], R. Calabrese[26,m], S. Calderon Ramirez[9], L. Calefice[45], M. Calvi[31,p], M. Calvo Gomez[46], P. Camargo Magalhaes[2,a], J.I. Cambon Bouzas[47], P. Campana[28], D.H. Campora Perez[82], A.F. Campoverde Quezada[7], S. Capelli[31], M. Caporale[25], L. Capriotti[26], R. Caravaca-Mora[9], A. Carbone[25,k], L. Carcedo Salgado[47], R. Cardinale[29,n], A. Cardini[32], I. Carli[5], P. Carniti[31], L. Carus[22], A. Casais Vidal[65], R. Caspary[22], G. Casse[61], M. Cattaneo[49], G. Cavallero[26], V. Cavallini[26,m], S. Celani[22], I. Celestino[35,t], S. Cesare[30,o], A.J. Chadwick[61], I. Chahrour[87], H. Chang[4,d], M. Charles[16], Ph. Charpentier[49], E. Chatzianagnostou[38], R. Cheaib[79], M. Chefdeville[10], C. Chen[56], J. Chen[50], S. Chen[5], Z. Chen[7], M. Cherif[12], A. Chernov[41], S. Chernyshenko[53], X. Chiotopoulos[82], V. Chobanova[84], M. Chrzaszcz[41], A. Chubykin[44], V. Chulikov[28,36,49], P. Ciambrone[28], X. Cid Vidal[47], G. Ciezarek[49], P. Cifra[38], P.E.L. Clarke[59], M. Clemencic[49], H.V. Cliff[56], J. Closier[49], C. Cocha Toapaxi[22], V. Coco[49], J. Cogan[13], E. Cogneras[11], L. Cojocariu[43], S. Collaviti[50], P. Collins[49], T. Colombo[49], M. Colonna[19], A. Comerma-Montells[45], L. Congedo[24], J. Connaughton[57], A. Contu[32], N. Cooke[60], G. Cordova[35,t], C. Coronel[66], I. Corredoira[12], A. Correia[16], G. Corti[49],

JHEP01(2026)159

J. Cottee Meldrum[55], B. Couturier[49], D.C. Craik[51], M. Cruz Torres[2,h],
E. Curras Rivera[50], R. Currie[59], C.L. Da Silva[68], S. Dadabaev[44], L. Dai[72], X. Dai[4],
E. Dall'Occo[49], J. Dalseno[84], C. D'Ambrosio[62], J. Daniel[11], P. d'Argent[24], G. Darze[3],
A. Davidson[57], J.E. Davies[63], O. De Aguiar Francisco[63], C. De Angelis[32,l],
F. De Benedetti[49], J. de Boer[38], K. De Bruyn[81], S. De Capua[63], M. De Cian[63,49],
U. De Freitas Carneiro Da Graca[2,b], S. De Keijzer[38], E. De Lucia[28], J.M. De Miranda[2],
L. De Paula[3], M. De Serio[24,i], P. De Simone[28], F. De Vellis[19], J.A. de Vries[82],
F. Debernardis[24], D. Decamp[10], V. Dedu[13], S. Dekkers[1], L. Del Buono[16], B. Delaney[65],
H.-P. Dembinski[19], J. Deng[8], V. Denysenko[51], O. Deschamps[11], F. Dettori[32,l], B. Dey[79],
P. Di Nezza[28], I. Diachkov[44], S. Didenko[44], S. Ding[69], Y. Ding[50], L. Dittmann[22],
V. Dobishuk[53], A.D. Docheva[60], A. Doheny[57], C. Dong[4,d], A.M. Donohoe[23],
F. Dordei[32], A.C. dos Reis[2], A.D. Dowling[69], L. Dreyfus[13], W. Duan[73], P. Duda[83],
L. Dufour[49], V. Duk[34], P. Durante[49], M.M. Duras[83], J.M. Durham[68], O.D. Durmus[79],
A. Dziurda[41], A. Dzyuba[44], S. Easo[58], E. Eckstein[18], U. Egede[1], A. Egorychev[44],
V. Egorychev[44], S. Eisenhardt[59], E. Ejopu[61], L. Eklund[85], M. Elashri[66], J. Ellbracht[19],
S. Ely[62], A. Ene[43], J. Eschle[69], S. Esen[22], T. Evans[38], F. Fabiano[32], S. Faghih[66],
L.N. Falcao[2], B. Fang[7], R. Fantechi[35], L. Fantini[34,s], M. Faria[50], K. Farmer[59],
D. Fazzini[31,p], L. Felkowski[83], M. Feng[5,7], M. Feo[19], A. Fernandez Casani[48],
M. Fernandez Gomez[47], A.D. Fernez[67], F. Ferrari[25,k], F. Ferreira Rodrigues[3],
S. Ferreres Sole[38], M. Ferrillo[51], M. Ferro-Luzzi[49], S. Filippov[44], R.A. Fini[24],
M. Fiorini[26,m], M. Firlej[40], K.L. Fischer[64], D.S. Fitzgerald[87], C. Fitzpatrick[63],
T. Fiutowski[40], F. Fleuret[15], A. Fomin[52], M. Fontana[25], L.F. Foreman[63], R. Forty[49],
D. Foulds-Holt[59], V. Franco Lima[3], M. Franco Sevilla[67], M. Frank[49], E. Franzoso[26,m],
G. Frau[63], C. Frei[49], D.A. Friday[63,49], J. Fu[7], Q. Führing[19,g,56], T. Fulghesu[13],
G. Galati[24], M.D. Galati[38], A. Gallas Torreira[47], D. Galli[25,k], S. Gambetta[59],
M. Gandelman[3], P. Gandini[30], B. Ganie[63], H. Gao[7], R. Gao[64], T.Q. Gao[56], Y. Gao[8],
Y. Gao[6], Y. Gao[8], L.M. Garcia Martin[50], P. Garcia Moreno[45], J. García Pardiñas[65],
P. Gardner[67], K.G. Garg[8], L. Garrido[45], C. Gaspar[49], A. Gavrikov[33], L.L. Gerken[19],
E. Gersabeck[20], M. Gersabeck[20], T. Gershon[57], S. Ghizzo[29,n], Z. Ghorbanimoghaddam[55],
F.I. Giasemis[16,f], V. Gibson[56], H.K. Giemza[42], A.L. Gilman[66], M. Giovannetti[28],
A. Gioventù[45], L. Girardey[63,58], M.A. Giza[41], F.C. Glaser[14,22], V.V. Gligorov[16],
C. Göbel[70], L. Golinka-Bezshyyko[86], E. Golobardes[46], D. Golubkov[44], A. Golutvin[62,49],
S. Gomez Fernandez[45], W. Gomulka[40], I. Gonçales Vaz[49], F. Goncalves Abrantes[64],
M. Goncerz[41], G. Gong[4,d], J.A. Gooding[19], I.V. Gorelov[44], C. Gotti[31], E. Govorkova[65],
J.P. Grabowski[30], L.A. Granado Cardoso[49], E. Graugés[45], E. Graverini[50,u], L. Grazette[57],
G. Graziani[27], A.T. Grecu[43], L.M. Greeven[38], N.A. Grieser[66], L. Grillo[60], S. Gromov[44],
C. Gu[15], M. Guarise[26], L. Guerry[11], V. Guliaeva[44], P.A. Günther[22], A.-K. Guseinov[50],
E. Gushchin[44], Y. Guz[6,49], T. Gys[49], K. Habermann[18], T. Hadavizadeh[1],
C. Hadjivasiliou[67], G. Haefeli[50], C. Haen[49], S. Haken[56], G. Hallett[57], P.M. Hamilton[67],
J. Hammerich[61], Q. Han[33], X. Han[22,49], S. Hansmann-Menzemer[22], L. Hao[7],
N. Harnew[64], T.H. Harris[1], M. Hartmann[14], S. Hashmi[40], J. He[7,e], A. Hedes[63],
F. Hemmer[49], C. Henderson[66], R. Henderson[14], R.D.L. Henderson[1], A.M. Hennequin[49],
K. Hennessy[61], L. Henry[50], J. Herd[62], P. Herrero Gascon[22], J. Heuel[17], A. Heyn[13],

A. Hicheur[3], G. Hijano Mendizabal[51], J. Horswill[63], R. Hou[8], Y. Hou[11], D.C. Houston[60], N. Howarth[61], J. Hu[73], W. Hu[7], X. Hu[4,d], W. Hulsbergen[38], R.J. Hunter[57], M. Hushchyn[44], D. Hutchcroft[61], M. Idzik[40], D. Ilin[44], P. Ilten[66], A. Iniukhin[44], A. Iohner[10], A. Ishteev[44], K. Ivshin[44], H. Jage[17], S.J. Jaimes Elles[77,48,49], S. Jakobsen[49], E. Jans[38], B.K. Jashal[48], A. Jawahery[67], C. Jayaweera[54], V. Jevtic[19], Z. Jia[16], E. Jiang[67], X. Jiang[5,7], Y. Jiang[7], Y.J. Jiang[6], E. Jimenez Moya[9], N. Jindal[88], M. John[64], A. John Rubesh Rajan[23], D. Johnson[54], C.R. Jones[56], S. Joshi[42], B. Jost[49], J. Juan Castella[56], N. Jurik[49], I. Juszczak[41], D. Kaminaris[50], S. Kandybei[52], M. Kane[59], Y. Kang[4,d], C. Kar[11], M. Karacson[49], A. Kauniskangas[50], J.W. Kautz[66], M.K. Kazanecki[41], F. Keizer[49], M. Kenzie[56], T. Ketel[38], B. Khanji[69], A. Kharisova[44], S. Kholodenko[62,49], G. Khreich[14], T. Kirn[17], V.S. Kirsebom[31,p], O. Kitouni[65], S. Klaver[39], N. Kleijne[35,t], D.K. Klekots[86], K. Klimaszewski[42], M.R. Kmiec[42], T. Knospe[19], R. Kolb[22], S. Koliiev[53], L. Kolk[19], A. Konoplyannikov[6], P. Kopciewicz[49], P. Koppenburg[38], A. Korchin[52], M. Korolev[44], I. Kostiuk[38], O. Kot[53], S. Kotriakhova, E. Kowalczyk[67], A. Kozachuk[44], P. Kravchenko[44], L. Kravchuk[44], O. Kravcov[80], M. Kreps[57], P. Krokovny[44], W. Krupa[69], W. Krzemien[42], O. Kshyvanskyi[53], S. Kubis[83], M. Kucharczyk[41], V. Kudryavtsev[44], E. Kulikova[44], A. Kupsc[85], V. Kushnir[52], B. Kutsenko[13], J. Kvapil[68], I. Kyryllin[52], D. Lacarrere[49], P. Laguarta Gonzalez[45], A. Lai[32], A. Lampis[32], D. Lancierini[62], C. Landesa Gomez[47], J.J. Lane[1], G. Lanfranchi[28], C. Langenbruch[22], J. Langer[19], O. Lantwin[44], T. Latham[57], F. Lazzari[35,u,49], C. Lazzeroni[54], R. Le Gac[13], H. Lee[61], R. Lefèvre[11], A. Leflat[44], S. Legotin[44], M. Lehuraux[57], E. Lemos Cid[49], O. Leroy[13], T. Lesiak[41], E.D. Lesser[49], B. Leverington[22], A. Li[4,d], C. Li[4,d], C. Li[13], H. Li[73], J. Li[8], K. Li[76], L. Li[63], M. Li[8], P. Li[7], P.-R. Li[74], Q. Li[5,7], T. Li[72], T. Li[73], Y. Li[8], Y. Li[5], Y. Li[4], Z. Lian[4,d], Q. Liang[8], X. Liang[69], Z. Liang[32], S. Libralon[48], A.L. Lightbody[12], C. Lin[7], T. Lin[58], R. Lindner[49], H. Linton[62], R. Litvinov[32], D. Liu[8], F.L. Liu[1], G. Liu[73], K. Liu[74], S. Liu[5,7], W. Liu[8], Y. Liu[59], Y. Liu[74], Y.L. Liu[62], G. Loachamin Ordonez[70], A. Lobo Salvia[45], A. Loi[32], T. Long[56], F.C.L. Lopes[2,a], J.H. Lopes[3], A. Lopez Huertas[45], C. Lopez Iribarnegaray[47], S. López Soliño[47], Q. Lu[15], C. Lucarelli[49], D. Lucchesi[33,r], M. Lucio Martinez[48], Y. Luo[6], A. Lupato[33,j], E. Luppi[26,m], K. Lynch[23], X.-R. Lyu[7], G.M. Ma[4,d], H. Ma[72], S. Maccolini[19], F. Machefert[14], F. Maciuc[43], B. Mack[69], I. Mackay[64], L.M. Mackey[69], L.R. Madhan Mohan[56], M.J. Madurai[54], D. Magdalinski[38], D. Maisuzenko[44], J.J. Malczewski[41], S. Malde[64], L. Malentacca[49], A. Malinin[44], T. Maltsev[44], G. Manca[32,l], G. Mancinelli[13], C. Mancuso[14], R. Manera Escalero[45], F.M. Manganella[37], D. Manuzzi[25], D. Marangotto[30,o], J.F. Marchand[10], R. Marchevski[50], U. Marconi[25], E. Mariani[16], S. Mariani[49], C. Marin Benito[45], J. Marks[22], A.M. Marshall[55], L. Martel[64], G. Martelli[34], G. Martellotti[36], L. Martinazzoli[49], M. Martinelli[31,p], D. Martinez Gomez[81], D. Martinez Santos[84], F. Martinez Vidal[48], A. Martorell i Granollers[46], A. Massafferri[2], R. Matev[49], A. Mathad[49], V. Matiunin[44], C. Matteuzzi[69], K.R. Mattioli[15], A. Mauri[62], E. Maurice[15], J. Mauricio[45], P. Mayencourt[50], J. Mazorra de Cos[48], M. Mazurek[42], M. McCann[62], T.H. McGrath[63], N.T. McHugh[60], A. McNab[63], R. McNulty[23], B. Meadows[66], G. Meier[19], D. Melnychuk[42], D. Mendoza Granada[16], P. Menendez Valdes Perez[47], F.M. Meng[4,d],

JHEP01(2026)159

M. Merk[38,82], A. Merli[50,30], L. Meyer Garcia[67], D. Miao[5,7], H. Miao[7], M. Mikhasenko[78], D.A. Milanes[77,z], A. Minotti[31,p], E. Minucci[28], T. Miralles[11], B. Mitreska[19], D.S. Mitzel[19], R. Mocanu[43], A. Modak[58], L. Moeser[19], R.D. Moise[17], E.F. Molina Cardenas[87], T. Mombächer[49], M. Monk[57,1], S. Monteil[11], A. Morcillo Gomez[47], G. Morello[28], M.J. Morello[35,t], M.P. Morgenthaler[22], A. Moro[31,p], J. Moron[40], W. Morren[38], A.B. Morris[49], A.G. Morris[13], R. Mountain[69], H. Mu[4,d], Z.M. Mu[6], E. Muhammad[57], F. Muheim[59], M. Mulder[81], K. Müller[51], F. Muñoz-Rojas[9], R. Murta[62], V. Mytrochenko[52], P. Naik[61], T. Nakada[50], R. Nandakumar[58], T. Nanut[49], I. Nasteva[3], M. Needham[59], E. Nekrasova[44], N. Neri[30,o], S. Neubert[18], N. Neufeld[49], P. Neustroev[44], J. Nicolini[49], D. Nicotra[82], E.M. Niel[15], N. Nikitin[44], L. Nisi[19], Q. Niu[74], P. Nogarolli[3], P. Nogga[18], C. Normand[55], J. Novoa Fernandez[47], G. Nowak[66], C. Nunez[87], H.N. Nur[60], A. Oblakowska-Mucha[40], V. Obraztsov[44], T. Oeser[17], A. Okhotnikov[44], O. Okhrimenko[53], R. Oldeman[32,l], F. Oliva[59,49], E. Olivart Pino[45], M. Olocco[19], C.J.G. Onderwater[82], R.H. O'Neil[49], J.S. Ordonez Soto[11], D. Osthues[19], J.M. Otalora Goicochea[3], P. Owen[51], A. Oyanguren[48], O. Ozcelik[49], F. Paciolla[35,x], A. Padee[42], K.O. Padeken[18], B. Pagare[47], T. Pajero[49], A. Palano[24], L. Palini[30], M. Palutan[28], C. Pan[75], X. Pan[4,d], S. Panebianco[12], G. Panshin[5], L. Paolucci[63], A. Papanestis[58], M. Pappagallo[24,i], L.L. Pappalardo[26], C. Pappenheimer[66], C. Parkes[63], D. Parmar[78], B. Passalacqua[26,m], G. Passaleva[27], D. Passaro[35,t,49], A. Pastore[24], M. Patel[62], J. Patoc[64], C. Patrignani[25,k], A. Paul[69], C.J. Pawley[82], A. Pellegrino[38], J. Peng[5,7], X. Peng[74], M. Pepe Altarelli[28], S. Perazzini[25], D. Pereima[44], H. Pereira Da Costa[68], M. Pereira Martinez[47], A. Pereiro Castro[47], C. Perez[46], P. Perret[11], A. Perrevoort[81], A. Perro[49,13], M.J. Peters[66], K. Petridis[55], A. Petrolini[29,n], S. Pezzulo[29,n], J.P. Pfaller[66], H. Pham[69], L. Pica[35,t], M. Piccini[34], L. Piccolo[32], B. Pietrzyk[10], G. Pietrzyk[14], R.N. Pilato[61], D. Pinci[36], F. Pisani[49], M. Pizzichemi[31,p,49], V.M. Placinta[43], M. Plo Casasus[47], T. Poeschl[49], F. Polci[16], M. Poli Lener[28], A. Poluektov[13], N. Polukhina[44], I. Polyakov[63], E. Polycarpo[3], S. Ponce[49], D. Popov[7,49], S. Poslavskii[44], K. Prasanth[59], C. Prouve[84], D. Provenzano[32,l,49], V. Pugatch[53], G. Punzi[35,u], J.R. Pybus[68], S. Qasim[51], Q.Q. Qian[6], W. Qian[7], N. Qin[4,d], S. Qu[4,d], R. Quagliani[49], R.I. Rabadan Trejo[57], R. Racz[80], J.H. Rademacker[55], M. Rama[35], M. Ramírez García[87], V. Ramos De Oliveira[70], M. Ramos Pernas[57], M.S. Rangel[3], F. Ratnikov[44], G. Raven[39], M. Rebollo De Miguel[48], F. Redi[30,j], J. Reich[55], F. Reiss[20], Z. Ren[7], P.K. Resmi[64], M. Ribalda Galvez[45], R. Ribatti[50], G. Ricart[15,12], D. Riccardi[35,t], S. Ricciardi[58], K. Richardson[65], M. Richardson-Slipper[56], K. Rinnert[61], P. Robbe[14,49], G. Robertson[60], E. Rodrigues[61], A. Rodriguez Alvarez[45], E. Rodriguez Fernandez[47], J.A. Rodriguez Lopez[77], E. Rodriguez Rodriguez[49], J. Roensch[19], A. Rogachev[44], A. Rogovskiy[58], D.L. Rolf[19], P. Roloff[49], V. Romanovskiy[66], A. Romero Vidal[47], G. Romolini[26,49], F. Ronchetti[50], T. Rong[6], M. Rotondo[28], S.R. Roy[22], M.S. Rudolph[69], M. Ruiz Diaz[22], R.A. Ruiz Fernandez[47], J. Ruiz Vidal[82], J.J. Saavedra-Arias[9], J.J. Saborido Silva[47], S.E.R. Sacha Emile R.[49], N. Sagidova[44], D. Sahoo[79], N. Sahoo[54], B. Saitta[32,l], M. Salomoni[31,49,p], I. Sanderswood[48], R. Santacesaria[36], C. Santamarina Rios[47], M. Santimaria[28], L. Santoro[2], E. Santovetti[37], A. Saputi[26,49], D. Saranin[44], A. Sarnatskiy[81], G. Sarpis[49], M. Sarpis[80], C. Satriano[36,v],

A. Satta[37], M. Saur[74], D. Savrina[44], H. Sazak[17], F. Sborzacchi[49,28], A. Scarabotto[19], S. Schael[17], S. Scherl[61], M. Schiller[22], H. Schindler[49], M. Schmelling[21], B. Schmidt[49], N. Schmidt[68], S. Schmitt[65], H. Schmitz[18], O. Schneider[50], A. Schopper[62], N. Schulte[19], M.H. Schune[14], G. Schwering[17], B. Sciascia[28], A. Sciuccati[49], G. Scriven[82], I. Segal[78], S. Sellam[47], A. Semennikov[44], T. Senger[51], M. Senghi Soares[39], A. Sergi[29,n,49], N. Serra[51], L. Sestini[27], A. Seuthe[19], B. Sevilla Sanjuan[46], Y. Shang[6], D.M. Shangase[87], M. Shapkin[44], R.S. Sharma[69], I. Shchemerov[44], L. Shchutska[50], T. Shears[61], L. Shekhtman[44], Z. Shen[38], S. Sheng[5,7], V. Shevchenko[44], B. Shi[7], Q. Shi[7], W.S. Shi[73], Y. Shimizu[14], E. Shmanin[25], R. Shorkin[44], J.D. Shupperd[69], R. Silva Coutinho[2], G. Simi[33,r], S. Simone[24,i], M. Singha[79], N. Skidmore[57], T. Skwarnicki[69], M.W. Slater[54], E. Smith[65], K. Smith[68], M. Smith[62], L. Soares Lavra[59], M.D. Sokoloff[66], F.J.P. Soler[60], A. Solomin[55], A. Solovev[44], K. Solovieva[20], N.S. Sommerfeld[18], R. Song[1], Y. Song[50], Y. Song[4,d], Y.S. Song[6], F.L. Souza De Almeida[69], B. Souza De Paula[3], K.M. Sowa[40], E. Spadaro Norella[29,n], E. Spedicato[25], J.G. Speer[19], P. Spradlin[60], V. Sriskaran[49], F. Stagni[49], M. Stahl[78], S. Stahl[49], S. Stanislaus[64], M. Stefaniak[88], E.N. Stein[49], O. Steinkamp[51], H. Stevens[19], D. Strekalina[44], Y. Su[7], F. Suljik[64], J. Sun[32], J. Sun[63], L. Sun[75], D. Sundfeld[2], W. Sutcliffe[51], V. Svintozelskyi[48], P.N. Swallow[54], K. Swientek[40], F. Swystun[56], A. Szabelski[42], T. Szumlak[40], Y. Tan[4,d], Y. Tang[75], Y.T. Tang[7], M.D. Tat[22], J.A. Teijeiro Jimenez[47], A. Terentev[44], F. Terzuoli[35,x], F. Teubert[49], E. Thomas[49], D.J.D. Thompson[54], A.R. Thomson-Strong[59], H. Tilquin[62], V. Tisserand[11], S. T'Jampens[10], M. Tobin[5,49], T.T. Todorov[20], L. Tomassetti[26,m], G. Tonani[30], X. Tong[6], T. Tork[30], D. Torres Machado[2], L. Toscano[19], D.Y. Tou[4,d], C. Trippl[46], G. Tuci[22], N. Tuning[38], L.H. Uecker[22], A. Ukleja[40], D.J. Unverzagt[22], A. Upadhyay[49], B. Urbach[59], A. Usachov[39], A. Ustyuzhanin[44], U. Uwer[22], V. Vagnoni[25,49], V. Valcarce Cadenas[47], G. Valenti[25], N. Valls Canudas[49], J. van Eldik[49], H. Van Hecke[68], E. van Herwijnen[62], C.B. Van Hulse[47,aa], R. Van Laak[50], M. van Veghel[38], G. Vasquez[51], R. Vazquez Gomez[45], P. Vazquez Regueiro[47], C. Vázquez Sierra[84], S. Vecchi[26], J. Velilla Serna[48], J.J. Velthuis[55], M. Veltri[27,y], A. Venkateswaran[50], M. Verdoglia[32], M. Vesterinen[57], W. Vetens[69], D. Vico Benet[64], P. Vidrier Villalba[45], M. Vieites Diaz[47,49], X. Vilasis-Cardona[46], E. Vilella Figueras[61], A. Villa[25], P. Vincent[16], B. Vivacqua[3], F.C. Volle[54], D. vom Bruch[13], N. Voropaev[44], K. Vos[82], C. Vrahas[59], J. Wagner[19], J. Walsh[35], E.J. Walton[1,57], G. Wan[6], A. Wang[7], B. Wang[5], C. Wang[22], G. Wang[8], H. Wang[74], J. Wang[6], J. Wang[5], J. Wang[4,d], J. Wang[75], M. Wang[49], N.W. Wang[7], R. Wang[55], X. Wang[8], X. Wang[73], X.W. Wang[62], Y. Wang[76], Y. Wang[6], Y.H. Wang[74], Z. Wang[14], Z. Wang[30], J.A. Ward[57], M. Waterlaat[49], N.K. Watson[54], D. Websdale[62], Y. Wei[6], Z. Weida[7], J. Wendel[84], B.D.C. Westhenry[55], C. White[56], M. Whitehead[60], E. Whiter[54], A.R. Wiederhold[63], D. Wiedner[19], M.A. Wiegertjes[38], C. Wild[64], G. Wilkinson[64,49], M.K. Wilkinson[66], M. Williams[65], M.J. Williams[49], M.R.J. Williams[59], R. Williams[56], S. Williams[55], Z. Williams[55], F.F. Wilson[58], M. Winn[12], W. Wislicki[42], M. Witek[41], L. Witola[19], T. Wolf[22], E. Wood[56], G. Wormser[14], S.A. Wotton[56], H. Wu[69], J. Wu[8], X. Wu[75], Y. Wu[6,56], Z. Wu[7], K. Wyllie[49], S. Xian[73], Z. Xiang[5], Y. Xie[8], T.X. Xing[30], A. Xu[35,t], L. Xu[4,d], L. Xu[4,d], M. Xu[49], Z. Xu[49], Z. Xu[7], Z. Xu[5],

JHEP01(2026)159

K. Yang[62], X. Yang[6], Y. Yang[15], Z. Yang[6], V. Yeroshenko[14], H. Yeung[63], H. Yin[8], X. Yin[7], C.Y. Yu[6], J. Yu[72], X. Yuan[5], Y. Yuan[5,7], E. Zaffaroni[50], J.A. Zamora Saa[71], M. Zavertyaev[21], M. Zdybal[41], F. Zenesini[25], C. Zeng[5,7], M. Zeng[4,d], C. Zhang[6], D. Zhang[8], J. Zhang[7], L. Zhang[4,d], R. Zhang[8], S. Zhang[72], S. Zhang[64], Y. Zhang[6], Y.Z. Zhang[4,d], Z. Zhang[4,d], Y. Zhao[22], A. Zhelezov[22], S.Z. Zheng[6], X.Z. Zheng[4,d], Y. Zheng[7], T. Zhou[6], X. Zhou[8], Y. Zhou[7], V. Zhovkovska[57], L.Z. Zhu[7], X. Zhu[4,d], X. Zhu[8], Y. Zhu[17], V. Zhukov[17], J. Zhuo[48], Q. Zou[5,7], D. Zuliani[33,r], G. Zunica[28]

[1] *School of Physics and Astronomy, Monash University, Melbourne, Australia*
[2] *Centro Brasileiro de Pesquisas Físicas (CBPF), Rio de Janeiro, Brazil*
[3] *Universidade Federal do Rio de Janeiro (UFRJ), Rio de Janeiro, Brazil*
[4] *Department of Engineering Physics, Tsinghua University, Beijing, China*
[5] *Institute Of High Energy Physics (IHEP), Beijing, China*
[6] *School of Physics State Key Laboratory of Nuclear Physics and Technology, Peking University, Beijing, China*
[7] *University of Chinese Academy of Sciences, Beijing, China*
[8] *Institute of Particle Physics, Central China Normal University, Wuhan, Hubei, China*
[9] *Consejo Nacional de Rectores (CONARE), San Jose, Costa Rica*
[10] *Université Savoie Mont Blanc, CNRS, IN2P3-LAPP, Annecy, France*
[11] *Université Clermont Auvergne, CNRS/IN2P3, LPC, Clermont-Ferrand, France*
[12] *Université Paris-Saclay, Centre d'Etudes de Saclay (CEA), IRFU, Saclay, France, Gif-Sur-Yvette, France*
[13] *Aix Marseille Univ, CNRS/IN2P3, CPPM, Marseille, France*
[14] *Université Paris-Saclay, CNRS/IN2P3, IJCLab, Orsay, France*
[15] *Laboratoire Leprince-Ringuet, CNRS/IN2P3, Ecole Polytechnique, Institut Polytechnique de Paris, Palaiseau, France*
[16] *LPNHE, Sorbonne Université, Paris Diderot Sorbonne Paris Cité, CNRS/IN2P3, Paris, France*
[17] *I. Physikalisches Institut, RWTH Aachen University, Aachen, Germany*
[18] *Universität Bonn - Helmholtz-Institut für Strahlen und Kernphysik, Bonn, Germany*
[19] *Fakultät Physik, Technische Universität Dortmund, Dortmund, Germany*
[20] *Physikalisches Institut, Albert-Ludwigs-Universität Freiburg, Freiburg, Germany*
[21] *Max-Planck-Institut für Kernphysik (MPIK), Heidelberg, Germany*
[22] *Physikalisches Institut, Ruprecht-Karls-Universität Heidelberg, Heidelberg, Germany*
[23] *School of Physics, University College Dublin, Dublin, Ireland*
[24] *INFN Sezione di Bari, Bari, Italy*
[25] *INFN Sezione di Bologna, Bologna, Italy*
[26] *INFN Sezione di Ferrara, Ferrara, Italy*
[27] *INFN Sezione di Firenze, Firenze, Italy*
[28] *INFN Laboratori Nazionali di Frascati, Frascati, Italy*
[29] *INFN Sezione di Genova, Genova, Italy*
[30] *INFN Sezione di Milano, Milano, Italy*
[31] *INFN Sezione di Milano-Bicocca, Milano, Italy*
[32] *INFN Sezione di Cagliari, Monserrato, Italy*
[33] *INFN Sezione di Padova, Padova, Italy*
[34] *INFN Sezione di Perugia, Perugia, Italy*
[35] *INFN Sezione di Pisa, Pisa, Italy*
[36] *INFN Sezione di Roma La Sapienza, Roma, Italy*
[37] *INFN Sezione di Roma Tor Vergata, Roma, Italy*
[38] *Nikhef National Institute for Subatomic Physics, Amsterdam, Netherlands*
[39] *Nikhef National Institute for Subatomic Physics and VU University Amsterdam, Amsterdam, Netherlands*
[40] *AGH - University of Krakow, Faculty of Physics and Applied Computer Science, Kraków, Poland*
[41] *Henryk Niewodniczanski Institute of Nuclear Physics Polish Academy of Sciences, Kraków, Poland*
[42] *National Center for Nuclear Research (NCBJ), Warsaw, Poland*

JHEP01(2026)159

[43] *Horia Hulubei National Institute of Physics and Nuclear Engineering, Bucharest-Magurele, Romania*
[44] *Authors affiliated with an institute formerly covered by a cooperation agreement with CERN*
[45] *ICCUB, Universitat de Barcelona, Barcelona, Spain*
[46] *La Salle, Universitat Ramon Llull, Barcelona, Spain*
[47] *Instituto Galego de Física de Altas Enerxías (IGFAE), Universidade de Santiago de Compostela, Santiago de Compostela, Spain*
[48] *Instituto de Fisica Corpuscular, Centro Mixto Universidad de Valencia - CSIC, Valencia, Spain*
[49] *European Organization for Nuclear Research (CERN), Geneva, Switzerland*
[50] *Institute of Physics, Ecole Polytechnique Fédérale de Lausanne (EPFL), Lausanne, Switzerland*
[51] *Physik-Institut, Universität Zürich, Zürich, Switzerland*
[52] *NSC Kharkiv Institute of Physics and Technology (NSC KIPT), Kharkiv, Ukraine*
[53] *Institute for Nuclear Research of the National Academy of Sciences (KINR), Kyiv, Ukraine*
[54] *School of Physics and Astronomy, University of Birmingham, Birmingham, United Kingdom*
[55] *H.H. Wills Physics Laboratory, University of Bristol, Bristol, United Kingdom*
[56] *Cavendish Laboratory, University of Cambridge, Cambridge, United Kingdom*
[57] *Department of Physics, University of Warwick, Coventry, United Kingdom*
[58] *STFC Rutherford Appleton Laboratory, Didcot, United Kingdom*
[59] *School of Physics and Astronomy, University of Edinburgh, Edinburgh, United Kingdom*
[60] *School of Physics and Astronomy, University of Glasgow, Glasgow, United Kingdom*
[61] *Oliver Lodge Laboratory, University of Liverpool, Liverpool, United Kingdom*
[62] *Imperial College London, London, United Kingdom*
[63] *Department of Physics and Astronomy, University of Manchester, Manchester, United Kingdom*
[64] *Department of Physics, University of Oxford, Oxford, United Kingdom*
[65] *Massachusetts Institute of Technology, Cambridge, MA, United States*
[66] *University of Cincinnati, Cincinnati, OH, United States*
[67] *University of Maryland, College Park, MD, United States*
[68] *Los Alamos National Laboratory (LANL), Los Alamos, NM, United States*
[69] *Syracuse University, Syracuse, NY, United States*
[70] *Pontifícia Universidade Católica do Rio de Janeiro (PUC-Rio), Rio de Janeiro, Brazil, associated to* [3]
[71] *Universidad Andres Bello, Santiago, Chile, associated to* [51]
[72] *School of Physics and Electronics, Hunan University, Changsha City, China, associated to* [8]
[73] *Guangdong Provincial Key Laboratory of Nuclear Science, Guangdong-Hong Kong Joint Laboratory of Quantum Matter, Institute of Quantum Matter, South China Normal University, Guangzhou, China, associated to* [4]
[74] *Lanzhou University, Lanzhou, China, associated to* [5]
[75] *School of Physics and Technology, Wuhan University, Wuhan, China, associated to* [4]
[76] *Henan Normal University, Xinxiang, China, associated to* [8]
[77] *Departamento de Fisica, Universidad Nacional de Colombia, Bogota, Colombia, associated to* [16]
[78] *Ruhr Universitaet Bochum, Fakultaet f. Physik und Astronomie, Bochum, Germany, associated to* [19]
[79] *Eotvos Lorand University, Budapest, Hungary, associated to* [49]
[80] *Faculty of Physics, Vilnius University, Vilnius, Lithuania, associated to* [20]
[81] *Van Swinderen Institute, University of Groningen, Groningen, Netherlands, associated to* [38]
[82] *Universiteit Maastricht, Maastricht, Netherlands, associated to* [38]
[83] *Tadeusz Kosciuszko Cracow University of Technology, Cracow, Poland, associated to* [41]
[84] *Universidade da Coruña, A Coruña, Spain, associated to* [46]
[85] *Department of Physics and Astronomy, Uppsala University, Uppsala, Sweden, associated to* [60]
[86] *Taras Schevchenko University of Kyiv, Faculty of Physics, Kyiv, Ukraine, associated to* [14]
[87] *University of Michigan, Ann Arbor, MI, United States, associated to* [69]
[88] *Ohio State University, Columbus, United States, associated to* [68]

[a] *Universidade Estadual de Campinas (UNICAMP), Campinas, Brazil*
[b] *Centro Federal de Educacão Tecnológica Celso Suckow da Fonseca, Rio De Janeiro, Brazil*
[c] *Department of Physics and Astronomy, University of Victoria, Victoria, Canada*

[d] *Center for High Energy Physics, Tsinghua University, Beijing, China*
[e] *Hangzhou Institute for Advanced Study, UCAS, Hangzhou, China*
[f] *LIP6, Sorbonne Université, Paris, France*
[g] *Lamarr Institute for Machine Learning and Artificial Intelligence, Dortmund, Germany*
[h] *Universidad Nacional Autónoma de Honduras, Tegucigalpa, Honduras*
[i] *Università di Bari, Bari, Italy*
[j] *Università di Bergamo, Bergamo, Italy*
[k] *Università di Bologna, Bologna, Italy*
[l] *Università di Cagliari, Cagliari, Italy*
[m] *Università di Ferrara, Ferrara, Italy*
[n] *Università di Genova, Genova, Italy*
[o] *Università degli Studi di Milano, Milano, Italy*
[p] *Università degli Studi di Milano-Bicocca, Milano, Italy*
[q] *Università di Modena e Reggio Emilia, Modena, Italy*
[r] *Università di Padova, Padova, Italy*
[s] *Università di Perugia, Perugia, Italy*
[t] *Scuola Normale Superiore, Pisa, Italy*
[u] *Università di Pisa, Pisa, Italy*
[v] *Università della Basilicata, Potenza, Italy*
[w] *Università di Roma Tor Vergata, Roma, Italy*
[x] *Università di Siena, Siena, Italy*
[y] *Università di Urbino, Urbino, Italy*
[z] *Universidad de Ingeniería y Tecnología (UTEC), Lima, Peru*
[aa] *Universidad de Alcalá, Alcalá de Henares, Spain*
[†] *Deceased*

JHEP01(2026)159